

1 Outer approximation algorithm with physical domain  
2 reduction for computer-aided molecular and separation  
3 process design

4 Smitha Gopinath, George Jackson, Amparo Galindo, Claire S. Adjiman\*

Department of Chemical Engineering, Centre for Process Systems Engineering,

Imperial College London, South Kensington Campus, London SW7 2AZ, United Kingdom

c.adjiman@imperial.ac.uk

5 June 22, 2016

6 **Abstract**

7 Integrated approaches to the design of separation systems based on computer-  
8 aided molecular and process design (CAMPD) can yield an optimal solvent structure  
9 and process conditions. The underlying design problem, however, is a challenging  
10 mixed integer nonlinear problem (MINLP), prone to convergence failure as a result  
11 of the strong and nonlinear interactions between solvent and process. To facilitate  
12 the solution of this problem, a modified outer-approximation algorithm is proposed.  
13 Tests that remove infeasible regions from both the process and molecular domain are  
14 embedded within the outer-approximation framework. Four tests are developed to  
15 remove sub-domains where constraints on phase behaviour that are implicit in process  
16 models or explicit process (design) constraints are violated. The algorithm is applied  
17 to three case studies relating to the separation of methane and carbon dioxide at

18 high pressure. The process model is highly nonlinear, and includes mass and energy  
19 balances as well as phase equilibrium relations and physical property models based on  
20 a group-contribution version of the statistical associating fluid theory (SAFT- $\gamma$  Mie)  
21 and the GC<sup>+</sup> group contribution method for some pure component properties. A fully  
22 automated implementation of the proposed approach is found to converge successfully  
23 to a local solution in 30 problem instances. The results highlight the extent to which  
24 optimal solvent and process conditions are interrelated and dependent on process  
25 specifications and constraints. The robustness of the CAMPD algorithm makes it  
26 possible to adopt higher-fidelity nonlinear models in molecular and process design.

27 Keywords: Mixed-integer optimization, Molecular design, Absorption, Carbon dioxide cap-  
28 ture, SAFT equation of state

## 29 Introduction

30 The transformation of feedstocks to desired products in chemical processes involves the use  
31 of a large variety of processing materials<sup>1</sup> such as solvents, adsorbents, catalysts, and heat  
32 transfer fluids. Traditionally, the selection of processing materials and the design of the  
33 process (flowsheet, unit sizes, operating conditions) have been approached sequentially,<sup>2</sup>  
34 although, material and process decisions are in fact interdependent.<sup>2,3</sup> Choosing a process-  
35 ing material based on a few desirable physicochemical properties, in isolation from process  
36 performance considerations, can thus lead to poor decisions: for example, a solvent that  
37 exhibits high solubility and selectivity for the solute of interest may be too expensive to  
38 regenerate, compromising the economic viability of the process. Instead, a process-wide  
39 evaluation of the material is essential to identify choices that lead to better, or even opti-  
40 mal, process performance metrics such as reduced cost and environmental impact.<sup>4</sup> Given  
41 the potential benefits that can be derived from an integrated approach to material and  
42 process design, there has been growing interest in addressing computer-aided molecular

43 and process design (CAMPD) problems,<sup>5</sup> in which the design of processing materials or  
44 molecules and that of the process are considered simultaneously.

45 In general, a CAMPD problem can be posed as a mixed-integer nonlinear optimization  
46 problem, provided that predictive algebraic models are available to capture the impact  
47 of material/molecular structure on relevant physicochemical properties, and the effect of  
48 these properties on the appropriate unit operations. Discrete variables are used to represent  
49 molecular-level decisions such as the number of groups of a given kind (for example, how  
50 many hydroxyl (OH) groups the optimal molecule contains, if any), with constraints used  
51 to specify how the groups can be combined.<sup>6,7,8,9</sup> Discrete variables can also be used to  
52 represent the connectivity between the groups,<sup>10,11</sup> and the identity of components if the  
53 material of interest is a mixture.<sup>12,13,14</sup>

54 The CAMPD problem is inherently more complex than the corresponding process de-  
55 sign problem with fixed material choices. Firstly, the presence of discrete choices makes the  
56 problem combinatorial in nature. Secondly, the design problem is highly nonlinear: many  
57 of the models that relate structural information to physical properties, such as the UNI-  
58 QUAC functional-group activity coefficients (UNIFAC) model<sup>15</sup> or the group contribution  
59 statistical associating fluid theory with a Mie potential (SAFT- $\gamma$  Mie) equation of state,<sup>16</sup>  
60 are non-convex, making it more challenging for local solvers to converge to the global min-  
61 imum or even a good solution. This is compounded by the fact that the identification of  
62 a feasible point for the process model for given values of the design variables can be chal-  
63 lenging from a numerical perspective in the absence of a good initial guess. Thirdly, there  
64 usually exist combinations of the discrete variables that satisfy all molecular design con-  
65 straints but that make the process model infeasible, because many implicit phase-behaviour  
66 constraints must be satisfied for the successful solution of a process model. For instance,  
67 in the case of a solvent-based gas separation process, the process is infeasible if the discrete  
68 variables represent a solvent that is in the vapour phase at inlet conditions (temperature  
69 and pressure). A more challenging implicit constraint is that both the vapour and liquid

70 phases must coexist at equilibrium across the entire set of operating conditions of the sep-  
71 aration unit. Process models are usually derived assuming that this behaviour holds, a  
72 reasonable assumption when all materials are fixed. In the context of CAMPD, however,  
73 the violation of these implicit constraints on fluid-phase behaviour is likely to, and often  
74 leads to, numerical failure. Even if the nonlinear equation solver converges, the solution is  
75 usually physically meaningless in such cases. Furthermore, constraints on phase behaviour  
76 are inherently discontinuous,<sup>17</sup> and can thus result in the failure of the optimization solver  
77 unless they are handled specifically. One strategy to address these discontinuities is to in-  
78 corporate them explicitly in the process model through the use of disjunctions<sup>18</sup> or through  
79 the use of complementarity constraints.<sup>19</sup> Such formulations, however, can require a greater  
80 number of discrete variables and can increase the complexity of process models. Another  
81 recently proposed strategy to deal with model discontinuities arising from a change in the  
82 number of phases is to carry out phase stability and equilibrium calculations for each stage  
83 via an external function.<sup>20</sup> The effective handling of these implicit constraints remains an  
84 active area of research.

85 Given these significant challenges, several methodologies have been proposed for the  
86 solution of CAMPD problems. One approach is the reformulation of the problem as a  
87 continuous nonlinear optimization problem. This can sometimes be achieved by placing  
88 restrictions on the types of materials that can be designed. For instance, Pereira et al.<sup>5</sup>  
89 considered the simultaneous design of a blend of *n*-alkanes and the corresponding absorp-  
90 tion process for the removal of carbon dioxide from a methane stream. Another way to  
91 develop a continuous optimization formulation at the process level is to optimize process  
92 performance in the space of molecular properties or descriptors in a first stage, leaving  
93 the identification of the optimal molecule or molecular structure for a second stage. In  
94 this vein, Eden et al.<sup>2</sup> proposed the formulation of a continuous process design problem  
95 to identify physical property targets, i.e., the values of the properties that give the best  
96 process performance. The concept of a “property cluster” was used to reduce the dimen-

97 sionality of the problem. These targets were then used in a computer-aided molecular  
98 design (CAMD) approach to find molecules that (nearly) achieve these targets. Within  
99 this class of approaches, the CAMD step can be performed via the use of “molecular  
100 property clusters”,<sup>21</sup> by using algebraic methods,<sup>22</sup> or molecular signatures.<sup>23</sup> In another  
101 method first proposed by Bardow et al.,<sup>24,25</sup> continuous molecular targeting (CoMT), the  
102 continuous descriptors of an optimal (hypothetical) solvent, representing the parameters  
103 of the PC-SAFT equation of state,<sup>26</sup> were first determined based on process performance.  
104 This was then used to identify an optimal molecule with similar descriptors, from a list  
105 of compounds<sup>25,27</sup> or more recently by deploying CAMD techniques to derive a CoMT-  
106 CAMD methodology.<sup>28</sup> These two-stage approaches can be seen as top-down strategies,  
107 since optimal process performance is sought first, and an appropriate molecular structure  
108 is then derived from this.

109 Other two-stage approaches can be viewed as bottom-up approaches in that they start  
110 from a molecular perspective and build up to an optimal process. The central idea is  
111 to reduce the combinatorial complexity of molecular design by first screening molecules  
112 from a wide design space, often using relatively simple property models and user-defined  
113 property targets, before using more demanding property and process models to evaluate  
114 the remaining options. This general methodology has been explored by several groups. The  
115 work of Karunanithi et al.<sup>29</sup> falls within this category, for example. In addition to screening  
116 based on property targets, Hostrup et al.<sup>3</sup> have used an analysis of phase diagrams, along  
117 with a metric of the driving force required for vapour-liquid separation to screen both  
118 molecular and separation process alternatives. Such a framework has been applied more  
119 recently to the design of ionic liquid entrainers for extractive distillation.<sup>30</sup> Approximate  
120 process models have also been used in the screening stage, for example by using targets  
121 on solvent selectivity and on process energy demand, as predicted with a shortcut model,  
122 to screen for entrainers.<sup>31</sup> The use of explicit property targets that are set based on prior  
123 knowledge or heuristics can, however, lead to the elimination of optimal solutions, just as

124 the use of approximate models can. An alternative to specified property targets is to set  
125 targets based on the preferred “direction” of each property, i.e., whether the property value  
126 should maximized or minimized. Multi objective optimization (MOO) techniques have  
127 been applied in this context, to identify molecules that lie on a Pareto front of physical  
128 property targets set by the designer based on insights into the process of interest. This  
129 smaller space of molecules, consisting of molecules in the Pareto set of solutions, can then  
130 be assessed further based on their performance in the process<sup>32,33</sup> or by using clustering  
131 of molecules to reduce the number of options.<sup>32,34,35,36</sup> An underlying assumption in such  
132 methods is that the optimal solution of the CAMPD problem lies on the Pareto front.  
133 However, this may not be the case if the objective function of the CAMPD problem does  
134 not vary monotonically with respect to each property or if the constraints of the CAMPD  
135 problem make some Pareto points infeasible. Another decomposition approach has been  
136 to optimize the structure of the molecule using a stochastic algorithm, whilst solving the  
137 process design problem with a gradient based algorithm for each structure generated.<sup>37</sup>

138 In both top-down and bottom-up two-stage methods, the solution obtained may differ  
139 from the solution of the fully integrated CAMPD problem. We note that in principle MOO  
140 based approaches offer a greater likelihood of identifying the solution than other approaches  
141 due to the absence of weights on the properties. In decomposing the problem, the strong  
142 interdependence between the process and molecular scales is represented in a simplified  
143 manner. In reality, several properties of the molecules or materials being designed play a  
144 role in determining the performance of the process and they do so in a nonlinear way, with  
145 unknown or indeed variable relative importance.<sup>25,35</sup> Furthermore, many of the molecu-  
146 lar/mixture properties vary with operating conditions, i.e., they are secondary properties  
147 in the sense discussed by Jaksland et al.<sup>38</sup> In turn the optimal operating conditions of the  
148 process, in turn, depend on the material that is chosen, as well as the process constraints  
149 and specifications. Even the feasible operating region depends on the material chosen: the  
150 range of temperatures and pressures at which a solvent is in the liquid state depends on its

151 molecular structure; some choices of molecular structure may lead to the appearance of new  
152 phases, perhaps due to immiscibility or partial miscibility between the various components  
153 in the process. The optimal solution of the full CAMPD problem therefore corresponds to  
154 a trade-off between different properties and process variables. In this closely interlinked  
155 multidimensional problem, the sequential design of a system consisting of the process and  
156 the processing materials, or molecules, may be sub-optimal.<sup>1</sup>

157 To address this issue, several solution methodologies for the integrated molecular and  
158 process design problem (the “full MINLP”) have been proposed. The main challenge  
159 arises from the highly nonlinear nature of the MINLP formulation that represents the  
160 integrated design problem. In the approach of Pereira et al.,<sup>5</sup> mentioned previously, the  
161 SAFT-VR SW equation of state<sup>39,40</sup> was used as a reliable and predictive model of the  
162 relevant thermodynamics. Although this model is highly nonlinear, the tractability of  
163 the problem was ensured by considering a continuous molecular design space. The direct  
164 solution of the MINLP arising from the CAMPD problem was adopted by Zhou et al.<sup>41</sup>  
165 to design a reactive process and the corresponding reaction solvent, including the recovery  
166 of the solvent from the reaction products by distillation. The complexity of the process  
167 model was tailored to make the problem tractable. In particular, the distillation column  
168 was modelled via a shortcut model and by assuming ideal vapour and liquid phases. The  
169 full CAMPD problem was also solved to design an extractive fermentation process and  
170 solvent,<sup>42</sup> based on a mixed-integer quadratic formulation. Initial guesses for the solution of  
171 the CAMPD using mixed integer sequential quadratic programming (MISQP)<sup>43</sup> algorithm  
172 were obtained by applying an evolutionary algorithm to solve the CAMPD. The integrated  
173 design of an organic Rankine cycle process conditions and working fluid was also solved  
174 as a “full MINLP” in recent work, facilitated by the fact that only pure component phase  
175 behaviour is of relevance in such a case.<sup>44</sup>

176 To handle more general design problems, one can adopt the approach of Buxton et al.<sup>8</sup>  
177 who modified the generalized Benders decomposition (GBD) algorithm<sup>45</sup>: they introduced

178 several steps prior to the solution of the primal problem, including a series of property tests  
179 that form a subset of the CAMD problem constraints, the initialization of various sets of  
180 equations in the process model, and mass-transfer feasibility tests, in which the process  
181 operating conditions were assumed to be fixed *a priori*. This approach was extended to  
182 tackle mixed-integer dynamic optimization problems,<sup>46</sup> to enable the simultaneous design  
183 of a batch process and the associated solvent. In these studies, the highly-nonlinear UNI-  
184 FAC model<sup>15</sup> was combined with the ideal gas equation to represent the relevant phase  
185 equilibria. The full solution of the CAMPD problem was also achieved by Burger et al.<sup>47</sup>  
186 based on a hierarchical optimization approach (HiOpt). In this case, simplified models  
187 of the process units were combined with rigorous thermodynamics using the SAFT- $\gamma$  Mie  
188 equation of state<sup>16</sup> and were used to optimize several performance metrics derived from the  
189 simplified process model. A multi-objective optimization algorithm was used to generate  
190 solutions that approximate the Pareto front of the MOO problem. These were then used  
191 as initial guesses for the solution of the full MINLP, which included detailed process and  
192 thermodynamic models. Thus, whereas MOO has been embedded in other approaches as  
193 a screening tool to reduce the size of the solution space, Burger et al.<sup>47</sup> used MOO to  
194 generate high-quality starting points to help overcome the inherent non-convexity of the  
195 problem, albeit without guarantee of global optimality. We note, however, that despite  
196 the useful initialization data that were produced by the solution of the MOO, the local  
197 solution of the full MINLP remained prone to initialization and convergence failures.

198 In our current contribution, we build on recent work<sup>48</sup> to propose a robust algorithm  
199 for the solution of the full MINLP. Several novel tests are embedded within a modified  
200 outer-approximation (OA)<sup>49,50</sup> algorithm to solve the MINLP, akin to the general princi-  
201 ple of integrating tests into a modified GBD algorithm deployed by Buxton et al.<sup>8</sup> and  
202 Giovanoglou et al.<sup>46</sup> The tests we develop differ from these earlier approaches, however, as  
203 the feasibility of the process is assessed for combinations of the values of the process *and*  
204 the molecular variables, rather than for values of the molecular variables only. When a new



205 solvent is generated at a major iteration of the modified OA algorithm, the tests help to  
206 ascertain the feasibility of using the solvent in the process, before solving the process opti-  
207 mization problem (primal problem) for the fixed solvent. The aim of the tests is two-fold:  
208 to determine *a priori* if a solvent is feasible in the process and, if it is, the ranges of values  
209 of the process variables for which it may be feasible. If the solvent is found to be infeasible  
210 throughout the process domain, it is removed from the search space without the need to  
211 evaluate the primal problem. If it is found to be feasible for some ranges of the variables  
212 only, these ranges define the “reduced process domain”. Through the tests we thus rec-  
213 ognize that the feasible process domain varies with the choice of solvent. In the screening  
214 methodology proposed here, unlike in previous work, molecules do not have to be screened  
215 at arbitrarily fixed operating conditions, but their feasibility may be evaluated across the  
216 process domain. A further useful output of the tests comes in the form of initial guesses  
217 for the optimization of the primal problem that lie in the reduced process domain and this  
218 is complemented by an initialization strategy that contributes to the overall robustness of  
219 the algorithm. In our current contribution, the tests are developed with a specific focus on  
220 solvent-based absorption processes; a similar approach can be followed for other separation  
221 processes, for example, liquid-liquid extraction.

222 The paper is organized as follows. In the next section, a motivating example is intro-  
223 duced to highlight more specifically the difficulties that must be overcome to solve CAMPD  
224 problems. The proposed tests are then developed in the methodology section and their in-  
225 tegration into the modified OA algorithm is discussed in the proposed CAMPD algorithm  
226 section. The application of the algorithm to several variants of the motivating example is  
227 investigated in the case studies section, where the effectiveness of the tests and the robust-  
228 ness of the algorithm are analyzed. Conclusions and perspectives are discussed in the final  
229 section of the paper.

## Motivating example

To illustrate the challenges inherent in CAMPD, we consider the following gas absorption design problem previously studied by Burger et al.<sup>47</sup>: *Given a flowsheet configuration for an absorption process, the composition  $\mathbf{y}_F$ , temperature  $T_F$ , and pressure  $P_F$  of the gaseous feed to be separated, and performance objectives and constraints, find the optimal values of the pressure in the absorber  $P_{abs}$ , the recycle flow rate of the solvent  $L_0$ , and the vector  $\mathbf{n}$  of numbers of groups of each type in the solvent.*

The flowsheet is shown in Figure 1. The feed to be separated comprises carbon dioxide and methane (as a simplification of a natural gas stream). The feed passes through an expansion valve and is contacted with a solvent in a counter current absorber with 10 stages. The treated gas leaving at the top of the absorber is required to have a methane purity of at least  $y_p$ . The spent solvent is regenerated at  $P_{flash} = 0.1$  MPa. The regenerated solvent is mixed with a pure solvent at temperature  $T_s = 298$  K to make up for solvent losses. The resulting solvent stream is then pumped back into the absorber at a flow rate  $L_0$ . The objective is to maximize the net present value of the process over a 15 year lifetime.

The models chosen to represent the thermodynamics of the mixtures in the process play an important role in determining the validity of the solutions obtained. In Burger et al.,<sup>47</sup> most thermodynamic properties were predicted using SAFT- $\gamma$  Mie<sup>16</sup>, a group contribution equation of state (EoS) that belongs to the family of SAFT EoSs.<sup>51,52,53,54</sup> A group contribution EoS, such as SAFT- $\gamma$  Mie, offers a computationally tractable way of predicting the properties of molecules based on their chemical composition as described by the number of occurrences of each type of group in the molecule. Although it is common in molecular design work to describe liquid phases with the well-established UNIFAC model,<sup>15</sup> SAFT - $\gamma$  Mie allows one to consider a continuous and consistent description of thermodynamic properties for the entire fluid region (i.e., gas and liquid) and provides accurate predictions of fluid phase behaviour at the high pressures relevant to this case

256 study. In addition the GC<sup>+</sup> method<sup>55</sup> was used to predict melting points and flash points,  
257 while the viscosity and surface tension were estimated using correlations.<sup>56,57</sup> More details  
258 of the process model and property models may be found in the papers by Burger et al.<sup>47</sup>  
259 and Pereira et al.<sup>5</sup>

260       Though the flowsheet considered is relatively simple, the solution of the CAMPD prob-  
261 lem is challenging. The implementation of the process model presented by Burger et al.<sup>47</sup>  
262 comprised 548 equations, excluding the equations related to the evaluation of thermody-  
263 namic functions (for example, enthalpy, chemical potential) with the SAFT- $\gamma$  Mie EoS.  
264 The phase-equilibrium equations, namely the equality of the chemical potentials of each  
265 component across all phases and the equality of pressure across all phases (and trivially the  
266 equality of temperature), were included explicitly in the model for each stage as no flash  
267 algorithm was available for use with SAFT- $\gamma$  Mie at the time the work was conducted. An  
268 added complication in this model is that the EoS is explicit in the space of temperature  
269  $T$ -volume  $V$ - mole fraction  $\boldsymbol{x}$  coordinates, whereas the process model is implemented in  
270  $T$ - $P$ - $\boldsymbol{x}$  coordinates, where  $P$  is the pressure. This nonlinear subset of equations may have  
271 several roots, the number of which is not known *a priori*. Hence, the initialization of the  
272 EoS with a good guess for the volume was often necessary to obtain a solution that satisfies  
273 phase equilibrium. In the HiOpt approach,<sup>47</sup> initial guesses were generated by solving a  
274 simplified formulation of the full CAMPD as a MOO problem, providing solvent candidates  
275 judged to be of high quality on the basis of the MOO criteria. Each solution was then used  
276 as a starting point to solve the full CAMPD with the default OA-based MINLP solver in  
277 gPROMS.<sup>58</sup> Of the six starting points generated, the full CAMPD problem was solved for  
278 only three starting points. Difficulties arise in particular when the nonlinear solver fails to  
279 find a feasible point during the solution of the primal problem. While it is expected for  
280 infeasible primal problems to be encountered, it may be that a feasible point exists but  
281 is not found due to nonlinearities. Furthermore, in the gPROMS modelling environment  
282 used in this and our current work, a sequential solution approach is adopted in solving

283 the primal problem so that the optimization takes place in the space of degrees of freedom  
 284 only. It is then important to find a feasible point for the process model equations (i.e., a  
 285 square system of nonlinear equations) and to obtain the gradients of the constraints with  
 286 respect to the degrees of freedom. Failed evaluations of the process model or its gradients  
 287 were found to occur during the course of optimizations from three starting points and  
 288 led to convergence failure. Thus, while the HiOpt approach yielded high-performance sol-  
 289 vent/process combinations, there is significant scope for further enhancement of robustness  
 290 and efficiency, which may in turn lead to improved local solutions of the CAMPD problem.

## 291 Proposed methodology

The general CAMPD problem may be formulated as follows:

$$\begin{aligned}
 & \min_{\mathbf{x}, \mathbf{n}} f(\mathbf{x}, \mathbf{n}) \\
 & \text{s.t. } \mathbf{h}(\mathbf{x}, \mathbf{n}) = 0 \\
 & \mathbf{g}(\mathbf{x}, \mathbf{n}) \leq 0 \tag{P} \\
 & \mathbf{C}\mathbf{n} \leq \mathbf{d} \\
 & \mathbf{x} \in \mathbf{X} \\
 & \mathbf{n} \in \mathbf{N}
 \end{aligned}$$

292 where  $\mathbf{x} \in \mathbf{X} \subset \mathbb{R}^c$  is a  $c$ -dimensional vector of continuous variables, and  $\mathbf{n} \in \mathbf{N} \subset \mathbb{Z}^{+q}$  is  
 293 a  $q$ -dimensional vector of non-negative integer variables, where  $n_i$  represents the number  
 294 of occurrences of group  $i$  in the molecule. The set of equations  $\mathbf{h} : \mathbf{X} \times \mathbf{N} \rightarrow \mathbb{R}^e$  represents  
 295 the process and property models.  $\mathbf{g} : \mathbf{X} \times \mathbf{N} \rightarrow \mathbb{R}^a$  represents design constraints.  
 296  $f : \mathbf{X} \times \mathbf{N} \rightarrow \mathbb{R}$  is the design objective. The set of linear equations  $\mathbf{C}\mathbf{n} \leq \mathbf{d}$  represents  
 297 molecular feasibility constraints and bounds on the vector  $\mathbf{n}$ .

298 In MINLP solution algorithms such as the outer-approximation algorithm<sup>49</sup> and the

299 generalized Benders decomposition<sup>45</sup>, a new combination of the integer variables is gener-  
300 ated at each major iteration by solving a mixed integer linear program (MILP), the master  
301 problem. In conventional implementations, this combination is used to formulate a non-  
302 linear optimization problem (NLP), the primal problem, by fixing all integer variables to  
303 their values at the solution of the master problem. Thus, the primal problem for CAMPD  
304 is a nonlinear process-design problem (for a fixed solvent), whose solution is non-trivial. In  
305 our study, a modified OA algorithm is proposed, whereby each integer variable combina-  
306 tion, corresponding to a different candidate solvent, is subjected to a series of tests prior  
307 to the solution of the primal problem, with the aim to facilitate its solution by removing  
308 infeasible points from the search space and by providing good initial values for key problem  
309 variables.

310 For a solvent  $\mathbf{n}^{(k)}$  generated at major iteration  $k$  of the outer-approximation algorithm,  
311 we denote the feasible region of the corresponding primal problem by  $\mathbf{X}^{FR(k)} = \{\mathbf{x} \in \mathbf{X} : \mathbf{h}(\mathbf{x}, \mathbf{n}^{(k)}) = 0, \mathbf{g}(\mathbf{x}, \mathbf{n}^{(k)}) \leq 0\}$ . The identification of the exact feasible region,  $\mathbf{X}^{FR(k)}$ , for  
312 each candidate solvent is a difficult problem in its own right, and the focus is placed on  
313 identifying a reduced process domain,  $\mathbf{X}^{R(k)}$ , such that  $\mathbf{X}^{FR(k)} \subseteq \mathbf{X}^{R(k)} \subset \mathbf{X}$ , by applying  
314 a series of tests. Thus, the tests are designed to overestimate the feasible region in order  
315 to avoid eliminating potential solutions. Only regions that can be detected *a priori* to be  
316 infeasible with respect to implicit and explicit process constraints are removed. This not  
317 only reduces the optimization search space, but also enhances the convergence of the solver  
318 during the solution of the primal problem. Furthermore, when  $\mathbf{X}^{R(k)} = \emptyset$  for a molecule  
319 it is removed from the search space using an integer cut, and the solution of the primal  
320 problem for this candidate solvent is avoided.

322 Four tests are used in our current study to identify (and thus exclude) infeasible regions  
323 in the domain. Test 0 is used to identify a subdomain in which the feed is in the desired  
324 phase and to tighten user-provided bounds on the process domain. This test is independent  
325 of the solvent and only needs to be applied once at the beginning of the algorithm. The

326 three other tests are applied at each iteration. Test 1 is used to determine whether the  
327 properties of the pure candidate solvent make it suitable for separation, i.e, whether the  
328 solvent is a liquid at process temperatures, is safe and is feasible to handle. Test 2 is used  
329 to eliminate pressures at which the solvent and feed fail to form a two-phase mixture. Test  
330 3 is used to eliminate pressures at which the treated gas leaving the absorber cannot be  
331 obtained at the required purity. If any of Tests 1, 2 or 3 are infeasible, the solvent is  
332 eliminated from the search. Tests 2 and 3 are posed as continuous nonlinear optimization  
333 problems. If these problems are feasible for the current solvent, they provide bounds as  
334 well as initial guesses for the solution of the primal problem. The information gained  
335 through the solution of the primal problem and the tests is used to formulate the next  
336 master problem and to generate a new solvent.

### 337 **Test 0: Inlet stream phase stability after isenthalpic expansion**

338 Feed streams in separation systems often undergo adjustments in conditions before entering  
339 a separation unit through temperature-change or pressure-change equipment. The aim of  
340 Test 0 is to identify the impact of these units on feasible conditions. Test 0 is described here  
341 by considering a gas stream undergoing an expansion. Consider a feed stream at pressure  
342  $P_F$ , temperature  $T_F$  and composition  $\mathbf{y}_F$  from which one component must be separated.  
343 The feed is expanded with an isenthalpic valve before entering an absorber with  $N$  stages.  
344 The pressure is thus reduced from  $P_F$  to the pressure  $P_{N+1}$  at the absorber inlet, as shown  
345 in Figure 1. User-defined ranges of allowable pressures and temperatures in the absorber  
346 are given by  $[P_{N+1}^L, P_{N+1}^U]$  and  $[T_{N+1}^L, T_{N+1}^U]$ . In Test 0, the aim is to find a subdomain in  
347 the space defined by these ranges over which the inlet stream to an absorber is stable. The  
348 test is applicable to mixtures with a positive Joule-Thomson coefficient under the relevant  
349 conditions, a requirement which commonly holds for gases at ambient temperatures. For  
350 instance, the Joule-Thomson coefficient of methane and carbon dioxide is positive at room

351 temperature over a wide range of pressures. The test is based entirely on a thermodynamic  
352 analysis of the feed stream alone and it is thus independent of the solvent.

353 A constraint implicit in most models of absorption columns is enforced in Test 0, namely  
354 that the stream to be separated must enter the absorber in the vapour phase. This is indeed  
355 necessary in practice for the feasible operation of the process. An evaluation of the process  
356 model may fail to converge when the stream at the vapour inlet of the absorber is in  
357 a two-phase state or is a liquid, which can imply there is no two-phase solution to the  
358 subset of equations that enforce vapour-liquid equilibrium in the column. Even if such an  
359 evaluation converges to the trivial solution of the phase-equilibrium equations, a change in  
360 the number of phases in the feed as the operating pressure changes during the solution of  
361 the primal problem introduces a discontinuity that usually causes the optimizer to fail to  
362 converge. Such discontinuities are averted by the using Test 0 as it identifies *a priori* the  
363 region of the process domain where the feed is in the gas phase.

364 To illustrate the development of Test 0, the dew point curve for a binary mixture of  
365 CO<sub>2</sub> and methane at fixed mole fraction of CO<sub>2</sub> of 0.8 is shown in Figure 2. The maximum  
366 temperature at which two phases can occur for a stream of fixed composition, which is  
367 referred to as the cricondentherm,  $T_{cr}$ , is indicated by the vertical arrow. We note that an  
368 isenthalpic expansion of a mixture with a positive Joule-Thomson coefficient, such as the  
369 mixture in Figure 2, results in a decrease in both pressure and temperature. Thus, when  
370  $P_{N+1} < P_F$ ,  $T_{N+1} < T_F$  must hold.

371 The phases that can exist in the valve outlet stream (points B in Figure 2), which  
372 corresponds to the inlet to the absorber, depend on the value of its temperature,  $T_{N+1}$ ,  
373 relative to  $T_{cr}$ . If  $T_{N+1}$  is greater than  $T_{cr}$ , the inlet to the absorber is in the gas phase.  
374 This is illustrated in Figure 2 for an isenthalpic expansion from A1 to B1. However, when  
375  $T_{N+1} \leq T_{cr}$ , two situations can occur depending on the value of the dew point pressure,  
376  $P_D$ , relative to the stream pressure,  $P_{N+1}$ : if  $P_{N+1} < P_D(T_{N+1}, \mathbf{y}_F)$ , the inlet stream is in  
377 the vapour region (expansion A2-B2 in Figure 2); if  $P_{N+1} \geq P_D(T_{N+1}, \mathbf{y}_F)$ , the expanded

378 stream is either in the two-phase or the liquid region (expansion A3-B3 in Figure 2).

379 In order to avoid the two-phase region altogether, in Test 0 we use  $T_{cr}$  to set a lower  
380 bound on the temperature of the absorber inlet stream as:

$$T_{N+1}^{L0} = \max(T_{cr}, T_{N+1}^L), \quad (1)$$

381 where the value of  $T_{cr}$  may be obtained from the iterative solution of an isothermal flash  
382 problem at  $y_F$  until a temperature is found for which no dew pressure exists. This lower  
383 bound on the temperature is then used to derive a lower bound on the absorber pressure  
384 by considering an isenthalpic expansion from  $(P_F, T_F)$  to temperature  $T_{N+1}^{L0}$ . The pressure  
385  $P_H$  following the expansion is obtained by equating the enthalpies at the inlet and outlet  
386 of the expansion valve:

$$H(P_F, T_F, \mathbf{y}_F) = H(P_H, T_{N+1}^{L0}, \mathbf{y}_F). \quad (2)$$

387 The minimum allowable pressure in the absorber may then be found as:

$$P_{N+1}^{L0} = \max(P_H, P_{N+1}^L). \quad (3)$$

388 A summary of Test 0 is given in Table 1. Unlike subsequent tests that depend on the  
389 solvent candidate  $\mathbf{n}^{(k)}$ , Test 0 is conservative in that it may remove some solutions at  
390 which  $T_{N+1} \leq T_{cr}$  and nonetheless the stream is in the vapour phase. If the solution of  
391 the CAMPD problem is found to be at the lower bound on temperature or pressure, these  
392 conservative bounds can be relaxed.

### 393 **Test 1: Solvent handling feasibility test**

394 The feasibility of employing a given molecule as the solvent in an absorption process is  
395 evaluated in Test 1 based on pure-component properties independently of the process under  
396 consideration. The properties that are evaluated in this test are “essential properties”, as



397 previously defined by Harper et al.<sup>59</sup> These constraints form part of the overall design  
 398 problem (P) and are an  $s$ -dimensional subset  $\mathbf{g}_1(\mathbf{n})$  of  $\mathbf{g}(\mathbf{x}, \mathbf{n})$  such that  $\mathbf{g}_1 : \mathbf{N} \rightarrow \mathbb{R}^s$ .  
 399 If they are linear, they are included in the master problem and therefore satisfied by the  
 400 candidate solvent, but otherwise only an approximation is included in the master problem  
 401 and the constraints may be violated by the candidate solvent. Because these constraints  
 402 are independent of the process conditions, they can readily be tested for feasibility before  
 403 solving the primal problem. Four constraints are described in our current work: failure  
 404 to meet any of these results in the elimination of the candidate molecule. Other process-  
 405 independent nonlinear pure-component property constraints can readily be included in  
 406 Test 1.

407 Prior to Test 1, the user specifies a solvent inlet temperature  $T_s$ , corresponding to the  
 408 temperature at which fresh solvent enters the process, and a desired temperature handling  
 409 range,  $[T_{sh}^L, T_{sh}^U]$ , corresponding to the temperatures at which the solvent may be stored  
 410 or transported, and which may depend on ambient conditions. For solvent handling to  
 411 be feasible, it is imperative for the solvent to be in the liquid state over the range of  
 412 temperatures:

$$[T_s^L, T_s^U] = [\min(T_{sh}^L, T_s), \max(T_{sh}^U, T_s)]. \quad (4)$$

413 It is generally expected that  $T_s \in [T_{sh}^L, T_{sh}^U]$ , but Eq. (4) ensures that the most appropriate  
 414 bounds are set if this is not the case. Given the monotonic dependence of saturated-vapour  
 415 pressure on temperature and the limited dependence of the melting line on pressure, a  
 416 solvent that remains liquid over  $[T_s^L, T_s^U]$  at atmospheric pressure can be assumed to remain  
 417 liquid at higher pressures (unless of course very high pressures are considered).

418 Hence, the first constraint in Test 1 is that the normal melting point  $T_{mp}$  of the solvent  
 419 is lower than  $T_s^L$ :

$$T_{mp}(P = 1 \text{ atm}, \mathbf{n}^{(k)}) < T_s^L. \quad (5)$$

420 Furthermore, the normal boiling point  $T_{bp}$  of the solvent must be greater than  $T_s^U$ , and

421 this is enforced by the second property constraint:

$$T_s^U - T_{bp}(P = 1 \text{ atm}, \mathbf{n}^{(k)}) < 0. \quad (6)$$

422 In addition to verifying the liquid range of the solvent, the safety of handling the solvent  
 423 is evaluated using its flash point  $T_{fp}$  at atmospheric pressure. The flash point must be  
 424 greater than  $T_s^U$ , as expressed by the third constraint in Test 1:

$$T_s^U - T_{fp}(P = 1 \text{ atm}, \mathbf{n}^{(k)}) < 0. \quad (7)$$

425 Finally, the last pure-component property criterion applied in this work is that the viscosity  
 426 of the solvent must not exceed  $\nu^U$ , the maximum viscosity that can be handled by the  
 427 pump in the absorption plant. Assuming that the viscosity increases monotonically with  
 428 decreasing temperature, it attains its maximum value at  $T_s^L$  for temperatures in the range  
 429  $[T_s^L, T_s^U]$ . Thus, the viscosity is evaluated at  $T_s^L$  in the fourth constraint in Test 1:

$$\nu(T_s^L, P = 1 \text{ atm}, \mathbf{n}^{(k)}) - \nu^U < 0. \quad (8)$$

430 In summary, Test 1 is an evaluation of problem (P1)

$$\begin{aligned} T_{mp}(P = 1 \text{ atm}, \mathbf{n}^{(k)}) - T_s^L &< 0 \\ T_s^U - T_{bp}(P = 1 \text{ atm}, \mathbf{n}^{(k)}) &< 0 \\ T_s^U - T_{fp}(P = 1 \text{ atm}, \mathbf{n}^{(k)}) &< 0 \\ \nu(T_s^L, P = 1 \text{ atm}, \mathbf{n}^{(k)}) - \nu^U &< 0 \end{aligned} \quad (\text{P1})$$

## 431 **Test 2: Separation feasibility test**

432 Test 2 is introduced to reduce the size of the process domain or of the molecular domain  
 433 based on the thermodynamic feasibility of the separation. No purity target is imposed,

434 other than the implicit constraint that the desired product leaves the absorber in the gas  
435 stream. Test 2 can be formulated for gas-liquid or liquid-liquid separations and is presented  
436 here in the context of gas absorption. For a given solvent  $\mathbf{n}^{(k)}$ , the test can be used to  
437 identify a value of the pressure on the bottom stage of the absorber above which separation  
438 is not feasible. If no such value can be found above the lower bound on absorber pressure,  
439 the solvent can be eliminated. The test is based on the fact that the coexistence of two  
440 phases on stage  $N$  is a necessary condition to effect any separation, since the inlet stream  
441 to be separated enters the absorber at stage  $N$  and the loaded solvent leaves from stage  
442  $N$ . Furthermore, from a modelling perspective, the presence of only one phase on stage  
443  $N$  (or on any stage of the absorber) results in a discontinuity that can lead to numerical  
444 difficulties and it is therefore desirable to avoid carrying out process optimization in such  
445 cases.

446 Consider a counter-current absorption column with  $N$  stages as shown in Figure 1. Let  
447 the composition, flowrate, and temperature of the vapour stream that leaves from a given  
448 stage  $j$  be represented by  $\mathbf{y}_j$ ,  $V_j$  and  $T_j$ , respectively and the composition, flowrate, and  
449 temperature of the liquid stream that leaves any stage  $j$  be represented by  $\mathbf{x}_j$ ,  $L_j$  and  $T_j$ ,  
450 respectively. The liquid stream entering the absorber on stage 1 is denoted by the subscript  
451 '0'. The following simplifying assumptions are made to develop the test:

- 452 1. The composition of the solvent stream entering the counter-current column (at stage  
453 1) is assumed to be known. In a process with solvent recycle, the exact composition  
454 of the solvent that enters the absorber is unknown. However, by assuming that the  
455 regeneration step leaves only small quantities of non-solvent components dissolved in  
456 the solvent, the composition of the solvent is set equal to that of a pure solvent for  
457 the purpose of this test alone. One may also argue that it must be feasible to operate  
458 the process with a pure solvent stream at plant start-up.
- 459 2. The feed to be treated is assumed to consist of two components only: the component

460 to be removed is referred to as the “solute” and the component to be purified as the  
 461 “product”. If the feed stream consists of more than two components, the proposed  
 462 test can be applied based on the two main components to be separated.

463 3. Stage  $N$  of the absorber is assumed to be an equilibrium stage.

We note that it is not necessary to assume that the two-phase region at given temperature and pressure is convex. The concepts of operating lines and difference points, developed for the design of ternary extraction systems by Hunter and Nash,<sup>60</sup> and discussed in Henley et al.,<sup>61</sup> are used in Test 2 to infer the conditions at which the separation is feasible. The difference point is a hypothetical stream<sup>60</sup> with “flowrate”  $\Delta$  and “composition”  $\mathbf{d}$  that can be defined with respect to any stage  $j$  in the column based on the vapour stream entering stage  $j$  and the liquid stream leaving that stage. It can be shown through overall and component mass balances that  $\Delta$  and  $\mathbf{d}$  are independent of  $j$ . These variables are defined by the following equations:

$$\Delta = V_{j+1} - L_j, \quad \forall j = 0, \dots, N. \quad (9)$$

$$\Delta d_i = V_{j+1}y_{j+1,i} - L_jx_{j,i}, \quad \forall j = 0, \dots, N, \quad \forall i = 1 \text{ to } NC. \quad (10)$$

where  $NC$  is the total number of components. Note that a hypothetical stage corresponding to  $j = 0$  has been defined in these equations to represent the vapour stream leaving the column as  $V_1$  and the clean solvent stream entering the column as  $L_0$ . Combining equations (9) and (10), with  $j = 0$ , to eliminate  $\Delta$ , and using assumption 1 to set  $\mathbf{x}_0$  to the pure solvent composition,  $\mathbf{x}_s$ , one can derive the following relation:

$$y_{1,i} = x_{s,i}L_0/V_1 + d_i(1 - L_0/V_1), \quad \forall i = 1, \dots, NC. \quad (11)$$

464 Equation (11) indicates that  $\mathbf{y}_1$  lies on the line joining  $\mathbf{x}_s$  and  $\mathbf{d}$ . This is illustrated in  
 465 Figure 3 for a representative ternary phase diagram for  $\text{CO}_2$ , methane and propyl-methyl

466 ether as a solvent. In addition to  $\mathbf{x}_s$  and  $\mathbf{y}_1$ , points  $\mathbf{d}'$  and  $\mathbf{d}''$  are placed for convenience on  
 467 line  $\overleftrightarrow{\mathbf{y}_1\mathbf{x}_s}$ , on either side of the ternary diagram. To further analyze the locus of difference  
 468 points  $\mathbf{d}$ , two cases, shown as dashed lines in Figure 3, can be distinguished:

- 469 • When  $V_1$  is greater than or equal to  $L_0$ ,  $\Delta$  is non-negative and the ratio  $L_0/V_1$  is less  
 470 than or equal to one. Thus,  $\mathbf{y}_1$  must lie between  $\mathbf{d}$  and  $\mathbf{x}_s$ , or equivalently,  $\mathbf{d}$  must lie  
 471 on the open ray  $\overrightarrow{\mathbf{y}_1\mathbf{d}'}$ . The open ray is used to specify that the point  $\mathbf{y}_1$  itself does  
 472 not lie within the feasible locus of  $\mathbf{d}$ .
- Similarly, when  $V_1$  is less than  $L_0$ , then  $\Delta$  is negative and the locus of  $\mathbf{d}$  is the open  
 ray  $\overrightarrow{\mathbf{x}_s\mathbf{d}''}$ . This may be inferred by rearranging equation (11) as

$$x_{s,i} = y_{1,i}V_1/L_0 + d_i(1 - V_1/L_0), \quad \forall i = 1, \dots, NC. \quad (12)$$

473 Thus, the locus of  $\mathbf{d}$  consists of the two disconnected rays defined by excluding the closed  
 474 line segment  $\overline{\mathbf{y}_1\mathbf{x}_s}$  from line  $\overleftrightarrow{\mathbf{y}_1\mathbf{x}_s}$ .

The operating line for stage  $N$  may also be specified as

$$V_{N+1}y_{F,i} - L_Nx_{N,i} = \Delta d_i, \quad \forall i = 1 \dots NC. \quad (13)$$

475 It is apparent from equation(13) that  $\mathbf{y}_F$ ,  $\mathbf{x}_N$ , and  $\mathbf{d}$  are collinear. Since  $\mathbf{x}_N$  is the  
 476 composition of the liquid stream leaving stage  $N$ , from assumption 3, it must be a point on  
 477 the saturated-liquid curve and therefore line  $\overleftrightarrow{\mathbf{y}_F\mathbf{d}}$  must intersect with the saturated-liquid  
 478 curve. Thus, a necessary condition for absorption to be feasible is that the two-phase  
 479 region should be large enough for a point  $\mathbf{d}$  to exist such that  $\overleftrightarrow{\mathbf{y}_F\mathbf{d}}$  intersects the saturated  
 480 liquid curve at the stage pressure  $P_N$  and temperature  $T_N$ .

481 To define further the condition for which separation is feasible, consider the situation  
 482 when  $\overline{\mathbf{y}_F\mathbf{x}_s}$  is tangential to the saturated-liquid curve at  $\mathbf{x}_N$ , and does not intersect the  
 483 saturated-liquid curve at any other point on the curve.  $\theta$  is the angle the tangent makes

484 with the horizontal in the clockwise direction (as shown Figure 3). Line  $\overline{\mathbf{y}_F \mathbf{x}_s}$  is an infeasible  
 485 operating line as  $\mathbf{x}_s$  does not lie within the feasible locus of  $\mathbf{d}$ . Consider any other point  
 486 on the saturated-liquid curve,  $\mathbf{x}_N''$ . Let  $\overline{\mathbf{y}_F \mathbf{x}_N''}$  make an angle  $\theta''$  with the horizontal in  
 487 the clockwise direction. It is easy to visualize and infer that  $\theta'' > \theta$  and that  $\overline{\mathbf{y}_F \mathbf{x}_N''}$   
 488 intersects the line segment  $\overline{\mathbf{y}_1 \mathbf{x}_s}$  (at point  $\mathbf{o}''$  in Figure 3). However, such an operating line  
 489 is infeasible as the feasible locus of the difference point excludes the line segment  $\overline{\mathbf{y}_1 \mathbf{x}_s}$ .  
 490 Consider any operating line drawn with  $\theta' < \theta$ . Such an operating line is infeasible as  
 491 it fails to intersect the two-phase region. Thus, separation becomes infeasible if  $\overline{\mathbf{y}_F \mathbf{x}_s}$  is  
 492 tangential to the two-phase region. Using the arguments outlined above, separation is also  
 493 infeasible when the line  $\overline{\mathbf{y}_F \mathbf{x}_s}$  falls above the two-phase region, that is it does not intersect  
 494 (and is not even tangential) to the two-phase region. This analysis holds for different types  
 495 of phase diagrams and this is illustrated in Appendix A. Thus, there exists an operating  
 496 line that connects to the locus of feasible difference points and that intersects the two-phase  
 497 region if and only if the segment  $\overline{\mathbf{y}_F \mathbf{x}_s}$  cuts through the two-phase region. Test 2 is based  
 498 on searching for pressures at which this requirement is met.

499 Based on the analysis of difference points, Test 2 is formulated as a search for a max-  
 500 imum pressure  $P_N^{U(k)}$  at which the line connecting the feed composition  $\mathbf{y}_F$  and the pure  
 501 solvent  $\mathbf{x}_s$  intersects the two-phase region. If there is no such pressure, the separation is in-  
 502 feasible at all pressures and the solvent is removed from the search space. The optimization

503 problem is given by

$$\begin{aligned}
P_N^{U(k)} = & \max_{P_N, T_N, \mathbf{y}_N, \mathbf{x}_N} P_N \\
\text{s.t.} & \frac{y_{F,1} - x_{N,1}}{y_{F,2} - x_{N,2}} = \frac{y_{F,1} - x_{s,1}}{y_{F,2} - x_{s,2}} \\
& \mu_i^V(\mathbf{y}_N, T_N, P_N, \mathbf{n}^{(k)}) = \mu_i^L(\mathbf{x}_N, T_N, P_N, \mathbf{n}^{(k)}), \\
& \forall i = 1 \dots NC \\
& \|\mathbf{y}_N - \mathbf{x}_N\|_2 \geq \epsilon \\
& \sum_{i=1}^{NC} x_{N,i} = 1 \\
& \sum_{i=1}^{NC} y_{N,i} = 1 \\
& P_{N+1}^L - PD \leq P_N \leq P_{N+1}^U \\
& \max(T_{mp}(\mathbf{n}^{(k)}) + 10, T_N^L) \leq T_N \leq \min(T_F + 20, T_N^U) \\
& 0 \leq \mathbf{x}_N \leq 1 \\
& 0 \leq \mathbf{y}_N \leq 1
\end{aligned} \tag{P2}$$

504 where the first constraint defines a point  $\mathbf{x}_N$  on the segment  $\overline{\mathbf{y}_F \mathbf{x}_s}$ , and the second con-  
505 straint ensures this point is in equilibrium with a point  $\mathbf{y}_N$ , thereby lying on the two-phase  
506 boundary.  $\mu_i^L$  and  $\mu_i^V$  are the chemical potentials of component  $i$  in the liquid and vapour  
507 phases, respectively. The third constraint ensures that the composition vectors  $\mathbf{x}_N$  and  $\mathbf{y}_N$   
508 that are obtained are not trivial solutions to the phase-equilibrium equations by setting  $\epsilon$   
509 to be a small positive number. In posing Problem (P2), bounds are imposed on the pres-  
510 sure  $P_N$  and temperature  $T_N$ . If the maximum pressure drop across stage  $N$  is  $\Delta P$ , the  
511 lowest allowable value of the stage pressure  $P_N$  is  $P_{N+1}^L - \Delta P$ , where  $P_{N+1}^L$  is inherited from  
512 Test 0. In addition, an upper bound on  $P_N$  is given by  $P_N < P_{N+1} \leq P_{N+1}^U$ . The bounds  
513 on temperature can be set by the user as  $T_N^L$  and  $T_N^U$ , but constraints are also included  
514 to ensure that the lower bound is at least 10 K greater than the normal melting point of  
515 the solvent and the upper bound is at most 20 K greater than the feed temperature  $T_F$ .  
516 Problem (P2) can be challenging to solve because it is infeasible for some pressures and it

517 may thus be difficult to find a feasible direction from an infeasible point due to the high  
518 degree of nonlinearity of the problem. A more tractable reformulation of the problem is  
519 presented in Appendix B.

520 Since Test 2 is based on thermodynamic feasibility only, Problem (P2) does not require  
521 the composition  $\mathbf{y}_1$  of the treated gas stream to be specified and is based entirely on the  
522 feed specification. Furthermore, the condition of separation feasibility that is used here  
523 for a counter-current column is exactly the same as that for a single-stage separation unit.  
524 Separation in a single stage is possible when the total composition of a mixture formed by  
525 combining the feed and the solvent lies within the two-phase region.

### 526 **Test 3: Purification feasibility**

527 Most separation processes are designed with a constraint on the required purity of the  
528 treated stream, and in Test 3 a thermodynamic analysis is used to eliminate conditions  
529 and solvents for which this constraint cannot be met. In the context of gas absorption,  
530 Test 3 can be used to find a lower bound  $P_1^{L(k)}$  on the operating pressure at the top of  
531 the absorber that ensures that the separation can yield a vapour stream with the required  
532 purity while using solvent  $\mathbf{n}^{(k)}$ . If the purity criterion is found to be infeasible within the  
533 known pressure bounds, solvent  $\mathbf{n}^{(k)}$  can be eliminated from the search space.

534 The temperature at stage 1 is denoted by  $T_1$ . The treated gas leaving the absorber  
535 with mole fractions  $\mathbf{y}_1$  is required to have a mole fraction  $y_{1,1}$  of product (component 1)  
536 of at least  $y_p$  and is assumed to be in equilibrium with a liquid stream that leaves stage  
537 1. A necessary condition for the purification to be feasible is thus that there exists an  
538 equilibrium point  $\mathbf{y}^*$  on the two-phase envelope such that the mole fraction of product  
539  $y_1^*$  is greater than or equal to  $y_p$  at some temperature and pressure. Thus, the feasibility  
540 of achieving the required degree of separation is evaluated based on an analysis of the  
541 vapour-liquid envelope in relation to a process design constraint on product purity,  $y_p$ .



542 The example of a mixture of CO<sub>2</sub>, methane, and propyl-methyl ether is used once again  
543 in Figures 4a and 4b to illustrate the test. The shaded region in the figures represents the  
544 area where the mole fraction of the methane product in the treated gas,  $y_{1,1}$ , meets or  
545 exceeds the minimum acceptable purity of  $y_p = 0.97$ . At a pressure of 0.1 MPa and  
546 a temperature of 270 K (Figure 4a), the vapour-liquid boundary does not intersect the  
547 feasible region. When the pressure is increased to 0.610 MPa, at the same temperature  
548 (Figure 4b), the saturated vapour curve passes through  $y_p = 0.97$ , indicating that a feasible  
549 pressure has been chosen.

550 In general, the test proposed here may be used to find the range of pressures over which  
551 the required purity criterion may be met. In our work, only a lower bound on pressure  
552 is sought by assuming the mole fraction of product (the purity) increases monotonically  
553 with pressure, i.e., if a pressure is found at which the purity criterion is satisfied, then it is  
554 assumed to be satisfied at all higher pressures. However, if at higher pressures the purity  
555 constraint cannot be met (see, for example, Figure 6b where the maximum purity that  
556 can be obtained decreases with an increase in pressure) the test overestimates the feasible

557 region. The test is formulated as follows:

$$\begin{aligned}
P_1^{L(k)} = & \min_{P_1, T_1, \mathbf{y}_1, \mathbf{x}_1} P_1 \\
\text{s.t.} & \mu_i^V(\mathbf{y}_1, T_1, P_1, \mathbf{n}^{(k)}) = \mu_i^L(\mathbf{x}_1, T_1, P_1, \mathbf{n}^{(k)}), \\
& \forall i = 1, \dots, NC \\
& \|\mathbf{y}_1 - \mathbf{x}_1\|_2 > \epsilon \\
& \sum_{i=1}^{NC} x_{1,i} = 1 \\
& \sum_{i=1}^{NC} y_{1,i} = 1 \\
& y_{1,1} \geq y_p \\
& 0 \leq \mathbf{x}_1 \leq 1 \\
& 0 \leq \mathbf{y}_1 \leq 1 \\
& P_1^L \leq P_1 \leq P_1^U \\
& \max(T_{mp}(\mathbf{n}^{(k)}) + 10, T_1^L) \leq T_1 \leq \min(T_1^U, T_F + 20)
\end{aligned} \tag{P3}$$

558 where  $\mathbf{x}_1$  represents the composition of the liquid in equilibrium with a gas of composition  
559  $\mathbf{y}_1$ .  $\mu_i^V$  and  $\mu_i^L$  represent the chemical potentials in the vapour and liquid phases, respec-  
560 tively. The first constraint ensures that two compositions on the vapour-liquid envelope  
561 are found. The second constraint is used as in Problem (P2) to ensure that  $\mathbf{x}_1$  and  $\mathbf{y}_1$  are  
562 distinct compositions at equilibrium rather than a trivial solution to the phase equilibrium  
563 equations. The bounds on pressure,  $P_1$ , can be derived from Test 2 based on the pressure  
564 drop model adopted. The bounds on temperature are set in a similar manner to those  
565 in Test 2. Convergence to the solution of Problem (P3), which is highly nonlinear, can  
566 be achieved by using an initial guess within the feasible region for the problem. At the  
567 solution, the purity constraint,  $y_{1,1} \geq y_p$ , is typically active, and the constraint ensuring  
568 a minimum separation between the two equilibrium points is inactive. Hence, an initial  
569 guess within the feasible region can circumvent difficulties arising from the high degree of  
570 nonlinearity of the problem. Another strategy for solving this problem is to reformulate it

571 as shown in Appendix C.

572 Finally, we note that the composition of the treated gas stream could of course be  
573 determined by solving the MESH equations for the  $N$  stages of the absorber. However,  
574 the use of Test 3 prior to such an evaluation allows a check to be performed based on the  
575 underlying phase-equilibrium model only, and it can lead to the *a priori* removal of regions  
576 of the domain where the purity constraint of the process cannot be met, without resorting  
577 to evaluating a more complex model.

## 578 **Proposed CAMPD algorithm**

### 579 **Overview of the algorithm**

580 The outer approximation algorithm<sup>49,50</sup> is modified to embed the tests presented in the  
581 previous sections. As in a standard outer-approximation framework, the primal and master  
582 problems are solved alternately. In the context of the general CAMPD problem (P),  
583 the primal problem at some iteration  $k$  consists of a process design problem for a fixed  
584 solvent  $\mathbf{n}^{(k)}$ . It is a continuous NLP that produces an upper bound on the optimal value  
585 of the objective function as well as information (optimal variable values and gradients  
586 and function values at the solution) that can be used to construct the master problem, a  
587 MILP. The solution of the master problem provides a lower bound on the optimal objective  
588 function and also yields a candidate solvent,  $\mathbf{n}^{(k+1)}$ , for the next iteration.

### 589 **Primal problem**

590 In the proposed algorithm, as shown in Figure 5, Test 0 is applied once at the start of  
591 the algorithm, yielding updated lower bounds on  $P_{N+1}$  and  $T_{N+1}$ . These bounds are used  
592 throughout the algorithm. At each major iteration  $k$  of the algorithm, Tests 1 to 3 are  
593 solved sequentially. If any of these tests is infeasible, the algorithm proceeds directly to the

594 solution of the master problem, which is formulated to embed some information from the  
595 failed test as described in detail in the next section on the master problem. If Test 1, Test  
596 2 and Test 3 are all feasible for solvent  $\mathbf{n}^{(k)}$ , the primal problem is solved following a two-  
597 step procedure which consists of initialization and solution. The initialization procedure  
598 is described further in Appendix D. Variable bounds for the primal problem are inherited  
599 from the solutions of Test 0, 2 and 3.

600 Before presenting the formulation of the primal problem, we note that the process and  
601 physical property models, as represented by equalities  $\mathbf{h}(\mathbf{x}, \mathbf{n}) = 0$  in Problem (P), are  
602 treated as implicit constraints in the solution approach developed here. Hence, the variable  
603 set  $\mathbf{x}$  is partitioned into a set of independent (decision) variables  $\mathbf{u}$  and a set of dependent  
604 variables  $\mathbf{x}^d$  so that  $\mathbf{x} = (\mathbf{u}, \mathbf{x}^d)^T$ . For fixed  $\mathbf{u}$  and  $\mathbf{n}$ ,  $\mathbf{h}(\mathbf{u}, \mathbf{x}^d, \mathbf{n}) = 0$  thus represents a  
605 square system of equations of dimension  $e \times e$  (cf. the definition of Problem (P)) that can  
606 equivalently be written as  $\mathbf{x}^d(\mathbf{u}, \mathbf{n})$ .

607 This leads to the following formulation of the primal problem:

$$\begin{aligned}
f^k = \min_{\mathbf{u}} \quad & f(\mathbf{u}, \mathbf{n}^{(k)}) \\
\text{s.t.} \quad & \mathbf{g}_2(\mathbf{u}, \mathbf{x}^d(\mathbf{u}, \mathbf{n}^{(k)}), \mathbf{n}^{(k)}) \leq 0 \\
& \mathbf{x}^{dL(k)} \leq \mathbf{x}^d(\mathbf{u}, \mathbf{n}^{(k)}) \leq \mathbf{x}^{dU(k)} \\
& \mathbf{u}^{L(k)} \leq \mathbf{u} \leq \mathbf{u}^{U(k)}
\end{aligned} \tag{P4}$$

608 where  $\mathbf{g}_2 \leq 0$  is the subset of inequality constraints obtained by removing the constraints  
609 used in Test 1 ( $\mathbf{g}_1 \leq 0$ ) from the overall set of inequality constraints  $\mathbf{g} \leq 0$  in Problem  
610 (P), the superscripts  $L$  and  $U$  denote lower and upper bounds respectively. The variable  
611 bounds may be specified by the user or inherited from the tests.

612 Furthermore, in the proposed formulation, the discrete choices corresponding to the  
613 number of groups of each type are represented by general integer variables rather than  
614 by binary variables as is common in the OA literature, with the exception of Fletcher

615 and Leyffer.<sup>50</sup> This leads to a smaller number of variables in the problem: the number of  
616 discrete variables is reduced because it is not necessary to express each integer variable as a  
617 function of several binary variables and there is no need to introduce additional continuous  
618 variables and equations to represent the number of groups as a function of the relevant  
619 binary variables. Consequently, fewer gradients need to be evaluated when solving the  
620 primal problem and deriving linearized constraints for the master problem.

### 621 **Master problem**

622 The exact formulation of the master problem depends on the outcome of Tests 1 to 3 and  
623 of (P4). If Tests 1, 2, and 3, and Problem (P4) are feasible, linearizations of the objective  
624 function and inequality constraints around the solution of the primal problem are added to  
625 the master problem. Several sets are defined in order to do so.  $A1^{(k)}$  is a set used to keep  
626 track of all active and violated constraints in Test 1. It contains pairs of indices  $(l, j)$ , where  
627 each  $j$  is the index of an active or violated constraint in (P1) at major iteration  $l$ , where  
628  $l \leq k$ . A set  $F^{(k)}$  is also defined such that each  $l \in F^{(k)}$  is the index of a major iteration  
629  $l \in \{1, \dots, k\}$  at which the primal was found to be feasible. For each  $l \in F^{(k)}$ , the value of  
630  $\mathbf{u}$  at the solution of the primal problem is denoted by  $\mathbf{u}^{(l)}$ , that is  $\mathbf{u}^{(l)} = \arg \min_{\mathbf{u}} f(\mathbf{u}, \mathbf{n}^{(l)})$ .  
631 Furthermore, the set  $A^{(k)}$  contains pairs of indices  $(l, m)$  where  $l \in F^{(k)}$  and each  $m$  is the  
632 index of an active constraint in  $g_2$  at the solution of Problem (P4) at major iteration  $l$ ,  
633 thereby keeping track of all active constraints in (P4) at successful solutions of the primal  
634 problem. A constraint is declared active if  $g_2(\mathbf{u}^{(l)}, \mathbf{n}^{(l)}) \geq \epsilon_a$ , where  $\epsilon_a$  is a small negative  
635 number (which is less than or equal to the feasibility tolerance). Finally, for each  $l \in F^{(k)}$ ,  
636 where  $l > 0$ , once the primal problem is solved, global convexity tests<sup>62</sup> are employed. The  
637 constraints in the set  $A^{(k)}$  of the master problem are evaluated with the integer variables  
638 fixed to  $\mathbf{n}^{(l)}$  and the continuous variables to the solution  $\mathbf{u}^{(l)}$ . If any of the constraints are  
639 violated, this indicates it is an invalid underestimator of the non-convex feasible region<sup>62</sup>,  
640 and hence it is removed from set  $A^k$ .

641 If one of the tests or the primal problem is infeasible, the recurrence of the infeasible  
 642 candidate solvent is prevented by introducing an integer cut in the master problem. There  
 643 are several ways to formulate such an integer cut. A commonly used approach in the  
 644 MINLP literature is the constraint proposed by Duran and Grossmann<sup>49</sup>, which applies to  
 645 binary variables only, and therefore cannot be applied to our formulation. A more general  
 646 approach to integer cuts, which does not require the discrete variables to be binary, has  
 647 been developed by Fletcher and Leyffer.<sup>50</sup> It involves the solution of a feasibility problem,  
 648 a continuous optimization problem in which the discrete variables are fixed to the values  
 649 corresponding to the infeasible combination. In the feasibility problem, the objective to be  
 650 minimized is the violation of the infeasible constraints, subject to the feasible constraints  
 651 of the problem. Linearizations of the violated constraints at the solution of the feasibility  
 652 problem may then be added to the master problem, to prevent recurrence of an infeasible  
 653 combination. While this approach is general, the need to solve an additional optimization  
 654 problem increases the computational cost. Thus, this is only applied to the constraints in  
 655 Test 1, when Test 1 is infeasible. Since there are no continuous decision variables in (P1),  
 656 linearizations of the violated constraints in Test 1 with respect to the integer variables can  
 657 be added to the master problem without having to solve a nonlinear optimization problem.

658 If one of Test 2, Test 3, or (P4) is infeasible, however, an integer cut based on the “Big-  
 659 M” approach is added to the master problem for all subsequent iterations to remove the  
 660 infeasible solvent. An integer cut is also applied if the master problem generates an integer  
 661 combination that has previously been found to be feasible in problem (P4). Such a cut is not  
 662 added at every iteration to prevent an unnecessary increase in the number of constraints and  
 663 auxiliary variables. To formulate the integer cut, the set  $IC^{(k)}$  is introduced to keep track  
 664 of all major iterations  $l$  at which Test 2, Test 3 or the primal (P4) is infeasible ( $l \leq k$ ), or  
 665 at which the solution to the master problem  $\mathbf{n}^{(l+1)}$  is a repetition of a previously generated  
 666 (feasible) integer combination, i.e., there exists  $l'$  such that  $\mathbf{n}^{(l')} = \mathbf{n}^{(l+1)}$ ,  $l' \leq l \leq k$ . The

667 set of integer cuts takes the following form:

$$M^L(1 - y_l) + \epsilon_c \leq \sum_{i=1}^q \left( b^{i-1} \left( n_i - n_i^{(l)} \right) \right) \leq M^U y_l - \epsilon_c, \quad \forall l \in IC^{(k)}, \quad (14)$$

668 where the vector  $\mathbf{n}$ , with elements  $n_i$ , describes the solvent being sought in the master  
669 problem,  $M^L$  is a large negative number,  $M^U$  a large positive number,  $b$  is a constant  
670 set such that  $b > \max_{i=1, \dots, q} (n_i^U)$ ,  $\epsilon_c$  is a small positive number, and  $y_l$  is a binary variable  
671 introduced for iteration  $l$ , which ensures the central term is strictly positive or negative,  
672 but not equal to zero. The integer cut is applicable when each of the variables  $n_i$  is  
673 non-negative. We have used the sum of the products of  $n_i$  with powers of  $b$  to distinguish  
674 between two integer combinations. Alternatively, the sum of products of  $n_i$  with logarithms  
675 of prime numbers may be used as an integer cut.<sup>63</sup> Care must be taken in choosing  $M^L$  and  
676  $M^U$  to be of sufficiently large magnitude to prevent spurious infeasibilities, while ensuring  
677 that the MILP can be solved successfully.

678 Additional constraints are constructed if problem (P4) is found to be infeasible starting  
679 from  $\mathbf{u}_0^{(k)}$ , the initial guess to Problem (P4) at iteration  $k$ . First, an integer cut is con-  
680 structed for  $\mathbf{n}^{(k)}$  and added to the master problem. Furthermore, when a feasible solution  
681  $\left( \mathbf{u}_0^{(k)}, \mathbf{x}^{d(k)} \right)$  to the set of equations  $h(\mathbf{u}_0^{(k)}, \mathbf{x}^d, \mathbf{n}^{(k)}) = 0$  has been found, the objective  
682 function is linearized around  $\left( \mathbf{u}_0^{(k)}, \mathbf{n}^{(k)} \right)$  and added to the master problem. On the other  
683 hand, when no feasible solution to  $h(\mathbf{u}_0^{(k)}, \mathbf{x}^d, \mathbf{n}^{(k)}) = 0$  is found, no further information  
684 is included in the master problem. This approach ensures that the algorithm proceeds  
685 despite a failure to solve the process model without compromising convergence. The set  
686  $IF^{(k)}$  is defined as the set of iterations numbers  $l \leq k$  at which the primal (P4) was found  
687 to be infeasible, but where a feasible solution to the set of equality constraints was found  
688 for solvent  $\mathbf{n}^{(l)}$ .

689 Finally, the master problem contains bounds on the molecular and process variables.  
690 Constraints  $C\mathbf{n} \leq \mathbf{d}$  also ensure that molecular feasibility rules such as the octet rule<sup>6</sup>

691 are satisfied by the molecule. The set of constraints that are required to be present is  
 692 often dictated by the representation of the solvent-design space in the property prediction  
 693 models. Molecular feasibility constraints are given in the case study section.

694 The formulation of the master problem at iteration  $k$  is given by

$$\begin{aligned}
 \eta^{(k)} = \min_{\mathbf{u}, \mathbf{n}, \eta, \mathbf{y}} \quad & \eta \\
 \text{s.t.} \quad & f(\mathbf{u}^{(l)}, \mathbf{n}^{(l)}) + \nabla_{\mathbf{n}}^T f(\mathbf{u}^{(l)}, \mathbf{n}^{(l)})[\mathbf{n} - \mathbf{n}^{(l)}] \\
 & \quad + \nabla_{\mathbf{u}}^T f(\mathbf{u}^{(l)}, \mathbf{n}^{(l)})[\mathbf{u} - \mathbf{u}^{(l)}] \leq \eta, \quad \forall l \in F^{(k)} \\
 & f(\mathbf{u}^{0(l)}, \mathbf{n}^{(l)}) + \nabla_{\mathbf{n}}^T f(\mathbf{u}^{0(l)}, \mathbf{n}^{(l)})[\mathbf{n} - \mathbf{n}^{(l)}] \\
 & \quad + \nabla_{\mathbf{u}}^T f(\mathbf{u}^{0(l)}, \mathbf{n}^{(l)})[\mathbf{u} - \mathbf{u}^{0(l)}] \leq \eta, \quad \forall l \in IF^{(k)} \\
 & g_{2,m}(\mathbf{u}^{(l)}, \mathbf{n}^{(l)}) + \nabla_{\mathbf{n}}^T g_{2,m}(\mathbf{u}^{(l)}, \mathbf{n}^{(l)})[\mathbf{n} - \mathbf{n}^{(l)}] \\
 & \quad + \nabla_{\mathbf{u}}^T g_{2,m}(\mathbf{u}^{(l)}, \mathbf{n}^{(l)})[\mathbf{u} - \mathbf{u}^{(l)}] \leq 0, \quad \forall (l, m) \in A^{(k)} \\
 & g_{1,j}(\mathbf{n}^{(l)}) + \nabla_{\mathbf{n}}^T g_{1,j}(\mathbf{n}^{(l)})[\mathbf{n} - \mathbf{n}^{(l)}] \leq 0, \quad \forall (l, j) \in A1^{(k)} \\
 & M^L(1 - y_l) + \epsilon_c \leq \sum_{i=1}^q \left( b^{i-1} \left( n_i - n_i^{(l)} \right) \right) \leq M^U y_l - \epsilon_c, \\
 & \quad \quad \quad \forall l \in IC^{(k)} \\
 & \eta^{(k-1)} \leq \eta \leq f^U - \epsilon_n \\
 & \mathbf{u}^L \leq \mathbf{u} \leq \mathbf{u}^U \\
 & C\mathbf{n} \leq \mathbf{d} \\
 & y_l \in \{0, 1\}, \quad \forall l \in IC^{(k)}
 \end{aligned} \tag{M}$$

695 where  $\eta^{(0)} = -\infty$ ,  $\epsilon_n$  is a small positive number, and  $f^U$  is the lowest known objective  
 696 function value.

## 697 Implementation

698 A fully automated implementation of the CAMPD algorithm presented in Figure 5 has been  
 699 developed in C++, with an interface to gPROMS ModelBuilder 4.1.0<sup>58</sup> for the specification  
 700 and solution of all the subproblems required to solve the primal problem, i.e., Test 0 (Table



701 1), Problem (P1), Problem (P2a) (the reformulation of Problem (P2) in Appendix B),  
702 Problem (P3a) (the reformulation of Problem (P3) in Appendix C), and Problem (P4).  
703 The gORUN functionality of ModelBuilder is used to launch the solution of each of the sub-  
704 problems as needed, using batch files. The solution files for each of the sub-problems are  
705 read and the required information extracted and transferred to subsequent problems. For  
706 instance, the bounds derived by solving Problem (P2a) are embedded in Problems (P3a)  
707 and (P4) using the Foreign Object feature in gPROMS. In the same manner, the solution  
708 of Problem (P3a) provides a lower bound on the pressure in (P4) via a Foreign Object.  
709 The default continuous nonlinear optimizer in gPROMS, which is based on sequential  
710 quadratic programming, is used to solve problems (P2a), (P3a), and (P4). No attempt  
711 has been made to use a deterministic global optimization solver due to the scale and high  
712 degree of nonlinearity of the case studies considered. Problem (M) is formulated within the  
713 C++ code and solved using Gurobi 6.1,<sup>64</sup> which comes with an inbuilt C++ interface. The  
714 gradients of the objective function and active inequality constraints with respect to the  
715 integer variables are calculated using first-order forward finite differences. At iterations  
716 where a feasible solution of the primal problem is found, the gradients of the objective  
717 function and active inequality constraints with respect to the continuous variables are  
718 obtained from the output of the gPROMS nonlinear optimizer. When the primal problem  
719 is infeasible, the gradients of the objective function with respect to the continuous variables  
720 are computed using first-order forward finite differences.

721 Several strategies are used within the implementation to enhance the robustness of  
722 the algorithm. While Tests 2 and 3 provide rigorous bounds on pressure if solved to  
723 global optimality, Problems (P2a) and (P3a) are non-convex optimization problems that  
724 are solved using a local optimization solver within the current implementation. Hence, the  
725 tests may cut off feasible regions of the process and solvent domain. Furthermore, Problem  
726 (P4) is also non-convex and may wrongly be found to be infeasible by a local solver. The  
727 likelihood of these issues arising is reduced in a practical way by taking a number of steps

728 in problem formulation and initialization. These are described in more detail in Appendix  
729 D, where the initialization problem (P4I), also implemented in gPROMS, may be found.  
730 We note that initialization is an important element of robustness but that approaches to  
731 initialization other than that proposed in Appendix D may be adopted.

## 732 Case studies

733 The flowsheet for the separation of carbon dioxide from natural gas that was described  
734 in the section (cf. Figure 1) is used to develop three case studies (C1, C2, and C3) and  
735 to explore the performance of the proposed methodology, in particular in terms of the  
736 effectiveness of the proposed tests and the robustness of the overall algorithm. Different  
737 specifications of the feed and process constraints are given in each case study, in recognition  
738 of the fact that natural gas streams vary with respect to concentration of CO<sub>2</sub>, well-  
739 head pressure, and temperature. Commercially-exploited natural gas has a wide range  
740 of concentrations of CO<sub>2</sub>: from 0 to 90 % CO<sub>2</sub>.<sup>65</sup> For instance, large natural gas basins  
741 have been found in China that contain 80 to 97% of CO<sub>2</sub>.<sup>66</sup> Indeed, the CO<sub>2</sub> content  
742 of a given field varies as a function of parameters such as drilling time and well depth.  
743 Similarly, the pressure  $P_F$  of the feed stream sent to the acid gas removal unit is affected  
744 by the natural gas processing steps, particularly whether the pressure is lowered for the  
745 separation of condensates from the gas. Although the specifications and constraints vary  
746 across the three case studies, the optimization variables remain the same, making it possible  
747 to investigate the effect of different specifications on the optimal solution.

748 Some assumptions are made in formulating the case studies. Although natural gas  
749 contains other hydrocarbons than methane, methane is used here as the key valuable  
750 component, so that the feed is a binary mixture of methane and carbon dioxide. It is  
751 further assumed that the pressure drop in the absorber is negligible, so that the absorber  
752 operates at a constant pressure  $P_{abs}$  with  $P_{abs} = P_{N+1} = P_j$ ,  $j = 0, \dots, N$ . The process

753 model, which is based on the MESH equations is that described by Pereira et al.<sup>5</sup> and  
 754 Burger et al.<sup>47</sup>. The degrees of freedom that are optimized are the absorber pressure  $P_{abs}$   
 755 the solvent flow rate  $L_0$  and the solvent structure  $\mathbf{n}$ . The objective to be maximized is the  
 756 net present value,  $NPV$ , of the carbon dioxide removal process over a 15-year period. The  
 757 variables and specifications for the case studies are shown in Tables 2 and 3, while values  
 758 assigned to constants that appear in (P2a), (P3a), and (M) are shown in Appendix D.

759 The space of possible solvents consists of linear compounds containing the groups  $\text{CH}_3$ ,  
 760  $\text{CH}_2$ ,  $\text{eO}$ , and  $\text{cO}$ , where  $\text{eO}$  and  $\text{cO}$  both consist of a single oxygen atom and are distin-  
 761 guished from one another by their position in the molecule.  $\text{eO}$  (end oxygen) describes  
 762 an oxygen atom when bonded to one  $\text{CH}_3$  and one  $\text{CH}_2$  group, and  $\text{cO}$  (central oxygen)  
 763 an oxygen atom when bonded to two  $\text{CH}_2$  groups.<sup>47</sup> The solvent design space includes  
 764 groups for which published interaction parameters with the components of the feed ( $\text{CO}_2$   
 765 and  $\text{CH}_4$ ) are available within the SAFT- $\gamma$  Mie framework. Based on the bounds used on  
 766 the molecular variables  $\mathbf{n}$ , a set of 109 molecules can be constructed. While this space  
 767 is relatively small, this set of groups provides sufficiently varied phase behaviour for a  
 768 proof-of-concept study and makes it possible to enumerate all solutions to investigate the  
 769 effectiveness of the proposed algorithm. The molecular feasibility constraints for this set  
 770 of molecules ensure that every central oxygen atom,  $n_{\text{cO}}$ , is in between two  $\text{CH}_2$  groups  
 771 to prevent the generation of molecules such as peroxides for which existing groups are  
 772 expected to be ill-suited. Thus, the following two requirements need to be met: a) if  $\text{cO}$   
 773 groups are present, the number of  $\text{cO}$  groups is less than that of  $\text{CH}_2$  groups, b) when  $n_{\text{CH}_2}$   
 774 is zero,  $n_{\text{cO}}$  is also zero. These conditions may be written compactly as

$$n_{\text{cO}} \leq n_{\text{CH}_2} - n_{\text{CH}_2}/n_{\text{CH}_2}^U. \quad (15)$$

775 Here,  $n_{\text{CH}_2}^U$  represents the maximum number of  $\text{CH}_2$  groups in the molecule. An end oxygen  
 776 group can only be present if a  $\text{CH}_2$  group is present. This may be written as the following

777 constraint:

$$n_{eO} \leq n_{CH_2} n_{eO}^U, \quad (16)$$

778

779 In order to carry out a systematic analysis of robustness, the three case studies are  
780 solved from the discrete starting points (solvent candidates) listed in Table 4. Initial  
781 guess IDs 1-6 were used as starting points for the CAMPD optimization of case study  
782 C1 in previous work<sup>47</sup> and have been repeated here for comparison. Solvent IDs 7-10 are  
783 introduced in the current work to test more extensively the effect of the initial guess on  
784 the solution procedure. Overall, the algorithm is applied to 30 different combinations of  
785 initial guesses and specifications.

786 The effectiveness of the tests is also investigated systematically over the entire solvent  
787 design space, and for the different specifications of the three case studies. Test 1 is applied  
788 to all solvents in the search space, Test 2 is only applied to solvents that pass Test 1,  
789 and Test 3 to solvents that pass Tests 1 and 2, in accordance with the sequential testing  
790 protocol used in the algorithm. Test 2 results in updating the upper bound on the absorber  
791 pressure for a solvent  $\mathbf{n}^{(k)}$  only if a value  $P_{abs}^{U(k)}$  that is lower than  $P_{abs}^U$ , the upper bound on  
792 pressure for the case study of interest, is found. Test 3 leads to an update of the pressure  
793 lower bound for a solvent  $\mathbf{n}^{(k)}$  only if a pressure  $P_{abs}^{L(k)}$  greater than  $P_{abs}^L$ , the lower bound  
794 identified in Test 0, is found. The values of the updated pressure bounds taken over all the  
795 solvents for which the pressure bounds have been successfully updated following Tests 2 or  
796 3 are analyzed for each case study. Finally, the number of solvents for which a given test  
797 is active is investigated; a test is “active” for a given solvent if it can reduce the solvent  
798 domain (i.e., eliminate the solvent) or the process domain for that solvent (i.e., identify  
799 the process to be infeasible or identify updated pressure bounds).

## 800 Application of tests to entire solvent space

### 801 Case study C1

802 Case study C1 is based on the process model and process constraints that were used in  
803 previous work.<sup>47</sup> The treated gas is required at a purity of 97 mol % of methane. The  
804 temperature in the flash drum is required to be 10 Kelvin above the melting point of the  
805 solvent. Other specifications used in case study C1 are summarized in Table 3.

806 The results of applying the tests to the specifications of this and other case studies  
807 are shown in Table 5. For case study C1, Test 0 yields the cricondentherm  $T_{cr}$  as 222 K  
808 and  $P_{abs}^L$  is unaffected at the relevant conditions. The performance of the other tests is  
809 shown in Table 5. Test 1 is the only test that results in the elimination of solvents for the  
810 specifications in this case study; it removes 19.3% of the search space.

### 811 Case study C2

812 In case study C2, the separation of methane from a stream that has a high CO<sub>2</sub> content (92  
813 mol %) is considered. The feed is available at a relatively high temperature of 340 K. The  
814 feed is assumed to be available through some compression or expansion process, which is  
815 outside the system boundary considered for this case study, at the absorber pressure  $P_{abs}$   
816 which is an optimization variable. A larger domain for the absorber pressure is considered  
817 in this process, namely  $0.1 \text{ MPa} \leq P_{abs} \leq 12.9 \text{ MPa}$ . An additional constraint is placed on  
818 the process: that the temperature on stage  $N$  remains less than or equal to 325 K. Other  
819 constraints remain the same as in case study C1 (cf. Table 3).

820 Test 0 is not relevant to case study C2 as there is no isenthalpic valve. The performance  
821 of each of the other tests for case study C2 is reported in Table 5. Tests 1 and 2 are both  
822 effective in this case. Test 2 produces an upper bound on pressure such that  $P_{abs}^{U(k)} \leq P_{abs}^U$   
823 for 20.5 % of the solvent search space that passes Test 1 (88 molecules), as shown in Table  
824 5.

### 825 **Case study C3**

826 In case study C3, a feed at an intermediate CO<sub>2</sub> concentration (50 mol %) is considered.  
827 The purity constraint is tightened: 99 mol % of methane is required in the treated gas  
828 stream. An additional temperature constraint is also imposed, in which temperature  $T_1$   
829 is required to be greater than or equal to 298 K. The upper bound on absorber pressure  
830  $P_{abs}^U$  is set equal to the pressure  $P_F$  of the feed. All other constraints remain the same as  
831 in case study C1.

832 Test 0 yields the cricondentherm  $T_{cr}$  as 260 K and  $P_{abs}^L$  is not updated by the test at  
833 conditions relevant to case study C3. The performance of each of the other tests for case  
834 study C3 can be seen in Table 5. Tests 1 and 3 are active in the case study, with Test 3  
835 leading to the elimination of one solvent and an increase in the lower bound on absorber  
836 pressure for nine solvents. The improved bound on pressure that is provided by Test 3  
837 results in a small reduction of the domain.

## 838 **Application of the CAMPD algorithm**

### 839 **Overview of results over 30 runs**

840 The proposed algorithm is applied to each of the three case studies from the ten starting  
841 points in Table 4. Throughout the discussion, average values relating to the performance  
842 are calculated as arithmetic means. All 30 runs converge successfully to locally optimal  
843 solutions. The results of applying the proposed algorithm to the case studies from the ten  
844 starting points are presented in Table 6 and the performance statistics are reported in Table  
845 7. In case study C1, the best found solvent is CH<sub>3</sub>O(CH<sub>2</sub>O)<sub>5</sub>CH<sub>3</sub>. The algorithm converges  
846 to the same solution from each of the starting points. This a significant improvement in  
847 robustness compared to that observed in previous work.<sup>47</sup> Convergence of the algorithm  
848 was previously achieved from only 3 out of 6 starting points when attempting to solve  
849 CAMPD case study C1 using a standard MINLP algorithm without applying any tests.

850 The solvent design space has been enumerated for case study C1 by solving an NLP for  
851 each solvent that passes Test 1. The best solution is found to be identical to that obtained  
852 with the proposed algorithm. Even with the relatively small design space, we note that  
853 the algorithm is remarkably effective at identifying a good solvent while evaluating only  
854 a small fraction (9.3%) of the space. This advantageous computational performance is  
855 expected to be even more marked when tackling problems with a larger design space.

856 The results of applying the algorithm to case study C2 from the 10 solvent starting  
857 points are also presented in Table 6. The non-convexity of the space is apparent in applying  
858 the algorithm to case study C2. The chemical composition of the best found solvent is  
859  $\text{CH}_3\text{O}(\text{CH}_2)_7\text{OCH}_2\text{OCH}_3$ . The algorithm converges to the highest *NPV* solution from  
860 only one starting point, and yields a high-performance solvent but with an *NPV* which  
861 is 7.5% lower, from six of the starting points. These two top ranking molecules differ  
862 in chemical structure by one oxygen atom, which highlights the strong interplay between  
863 solvent choices and process performance. Of the five solutions generated, four of these have  
864 the same number of  $\text{CH}_2$  groups. With initial guess 1, the algorithm converges in three  
865 iterations to one of the lowest ranking solutions, and non-convexity is detected at the third  
866 iteration by the global convexity test<sup>62</sup> that is implemented in the proposed algorithm.  
867 On average, primal evaluations are attempted for only 7.8% of the solvent design space for  
868 case study C2.

869 Finally, the outcome of the ten runs for case study C3 is presented in the last row of  
870 Table 6. The algorithm converges to the solution with the highest *NPV* from each of the  
871 starting points. The best found solvent is  $\text{CH}_3\text{O}(\text{CH}_2\text{O})_7\text{CH}_3$ . The average number of  
872 iterations, primal evaluations and their standard deviations attain their smallest value in  
873 case study as may be seen in Table 7. The results indicate that on an average 4.3% of  
874 solvents in the design space are explored by the algorithm to arrive at the solution. The  
875 primal problem is evaluated for a mere 2.8% of the solvent design space. It can be seen in  
876 Table 6 that the value of the optimal pressure is at its upper bound,  $P_{abs}^U$ , indicating that

877 a more profitable process may be possible at higher pressures, although designing such a  
878 process would require taking into account the cost of compressing the feed.

879 It is instructive to compare the solutions obtained in the three case studies. The top  
880 ranking solvent found by the algorithm for each case study, the corresponding optimal  
881 process degrees of freedom, and objective function value are reported in Table 6 in the  
882 row immediately below the name of each case study. As can be seen, significantly different  
883 optimal solvents and process degrees of freedom have been found in the three variants of  
884 the problem statement. The results confirm that a strong interaction exists between the  
885 process objective and the choice of solvent, process variables, process specifications and  
886 constraints.

887 Overall, we find the proposed algorithm exhibits robust performance in solving the  
888 CAMPD problem over 30 distinct optimization runs. The computational time taken to  
889 execute the tests is typically negligible compared to the CPU time required to solve the  
890 primal problem. As can be seen in Table 7 the algorithm explores 8.1% of the space of  
891 solvents on average in identifying a locally optimal solution. As discussed in the description  
892 of the algorithm, Tests 2 and 3 are only applied to molecules that pass Test 1. It is evident  
893 from Table 7 that different tests are active in each of the case studies. Whether a test is  
894 active, that is, useful in reducing the domain, cannot be predicted *a priori* and the tests  
895 therefore complement each other in increasing the robustness of the algorithm. The *a priori*  
896 detection of infeasibility arising from the choice of solvent molecule, which occurs chiefly  
897 due to Test 1, and in two cases due to Test 3, makes it possible to avoid expensive process  
898 evaluations and optimizations at infeasible points in 17.8% of all the major iterations  
899 carried out over the 30 distinct runs. The elimination of infeasible solvents is especially  
900 desirable during the first iterations of the MINLP solver: in these the optimizer has little  
901 information about the domain and may generate a number of poor solvent choices, leading  
902 to an increased risk of numerical failure and increased computational cost. In 16 out of 30  
903 runs, although the initial guess solvent passed Test 1, the solvent generated for the second



904 iteration failed Test 1. The impact of each test is investigated in more detail in the next  
905 section.

### 906 **Analysis of tests within the CAMPD algorithm**

907 The statistics on active test instances shown in Table 7 depend on the specific sequence  
908 of solvent candidates generated by the algorithm, which in turn depends on the problem  
909 specifications and starting point. As a result, in some cases the tests are found to be active  
910 in fewer instances than in the studies of the overall solvent space presented in the section  
911 on the application of tests to the entire search space: this is true for Test 3, which is most  
912 active in case study C3, in 6.4% of iterations, but which can in principle be active for 9.2%  
913 of the overall search space. Test 2 is active for 11.1% of iterations for case study C2 but  
914 can be active for 16.5% of the solvent design space. However, the reverse can also be true.  
915 For example, Test 1 is active for 29.8% of iterations in case study C3 but can eliminate up  
916 to 19.3% of the overall search space (21 out of a 109 solvents).

917 Test 0 is the only test which is never active; this is a result of the feed specifications  
918 set for each of the case studies (cf. Table 3). The potential of Test 0 to reduce the process  
919 domain for different specifications is demonstrated in Table 8, where three new sets of feed  
920 conditions are used. The cricondentherm is shown in the table, together with the lower  
921 bound on absorber pressure obtained after the application of Test 0; this bound is increased  
922 significantly compared to the initial value of 0.1 MPa.

923 Tests 1, 2, and 3 not only lead to a reduction in the size of the process-solvent domain  
924 but also aid in enhancing the convergence of the CAMPD algorithm. In conjunction with  
925 the initialization procedure used to find a starting point for the primal problem (Problem  
926 (P4I)), the tests thus increase the robustness of the CAMPD algorithm. Test 1 prevents  
927 premature termination of the algorithm by eliminating molecules that do not satisfy process  
928 constraint  $\mathbf{g}_1$  and that may lead to failure to solve the nonlinear model equations for some  
929 solvents that fail Test 1. For example, consider molecule  $\mathbf{n} = [2, 8, 2, 7]^T$ , which is generated

930 at the second major iteration for 19 out of the 30 runs. This molecule is predicted to have a  
931 normal melting of  $T_{mp}(\mathbf{n}) = 302$  K, and therefore to be a solid at  $T_s$ , under the conditions  
932 relevant to the three case studies. If the tests are not applied, and instead the molecule is  
933 used directly to fix the integer variables in the primal problem for case study C1, the  
934 NLP solver fails to converge and the solution of the primal problem is thus inconclusive. It  
935 is possible to investigate the effectiveness of the different constraints in problem (P1). In  
936 all the major iterations in which Test 1 is active, we found that the melting point constraint  
937 (P1) is violated in 57.8% of the runs, whereas the flash-point constraint is violated in 42.2%  
938 of the runs. The other two constraints are never active.

939 To illustrate the application of the tests in more detail, the fourth major iteration from  
940 case study C2, with initial guess ID 4 used as a starting point, is shown in Table 9. The  
941 candidate solvent passes Test 1. Both Test 2 and Test 3 are feasible and result in an updated  
942 upper bound on pressure. Indeed, absorber pressures between the updated pressure upper  
943 bound of 12.065 MPa and the initial pressure upper bound of 12.9 MPa are found to lead  
944 to failed process model evaluations. With the updated bounds, while the process model is  
945 evaluated successfully at the initial point, no solution that meets the design constraint is  
946 found so the primal problem is deemed infeasible. As a result, linearizations of the primal  
947 problem functions are constructed and incorporated in the master problem as described in  
948 the section on the proposed CAMPD algorithm.

949 In order to assess the impact of the non-convexity of Problems (P2a) and (P3a), we  
950 also verified the bounds obtained by the tests by constructing phase diagrams for a few  
951 solvent-CO<sub>2</sub>-CH<sub>4</sub> systems, for the example shown in Table 9 as well as in other cases. We  
952 used HELD,<sup>67</sup> an algorithm that can reliably solve constant temperature and pressure flash  
953 problems to determine stable equilibrium phases, and we constructed the relevant phase  
954 diagrams (including the diagrams in Figures 3 and 4). We found that even though we had  
955 used local solvers to arrive at the bounds on pressure, these bounds are consistent with  
956 the fluid phase-behaviour of the mixtures in all cases tested.

957 While infeasible solvents may be “fathomed thanks to the tests, the evaluation of the  
958 primal problem for other solvents can often fail. The use of an initialization strategy (here,  
959 in the form of Problem (P4I)) for the primal problem is an essential component of the  
960 proposed approach. Consider case study C3, with the initial guess of solvent structure  
961 set as follows:  $\mathbf{n}^{(0)} = [2, 5, 2, 4]^T$  (Initial guess ID 2, Table 4). Without taking any steps  
962 to identify a starting point for the process model, the standard MINLP solver terminates  
963 prematurely during its first iteration, in which  $\mathbf{n}$  is relaxed to a continuous variable. This  
964 is due to a failure to evaluate the process model, which is avoided when a starting point  
965 is generated with the initialization problem. In some cases, even when the initialization  
966 problem is infeasible because there is no feasible path between the initialization solvent  
967  $\mathbf{n}_0$  and corresponding initial values,  $\mathbf{u}_0$  and  $\mathbf{x}_0^d$ , and the desired solvent,  $\mathbf{n}^{(k)}$  and  $\mathbf{u}_0$ , the  
968 nonlinear optimization solver can succeed in identifying a solution to the primal problem.

## 969 Conclusions

970 A modified outer approximation algorithm is proposed to solve CAMPD problems for sep-  
971 aration systems, enabling the simultaneous optimization of solvent and process variables.  
972 The approach is developed to overcome the numerical challenges that arise due to the  
973 strong nonlinear interactions between process and solvent, with the aim to enhance ro-  
974 bustness and increase the likelihood of identifying high-performance solutions. Four tests  
975 are embedded within an outer approximation algorithm to reduce the domain of solvent  
976 and process variables before attempting to find an optimal set of process variables for a  
977 specified solvent by solving the primal problem. In Test 0, the effect of adjustments to  
978 the feed conditions on the feasible region of the process is quantified. Specifically, a lower  
979 bound is obtained on the pressure that can be achieved through the isenthalpic expansion  
980 of a stream with a positive Joule-Thomson coefficient. In Test 1, molecules which violate  
981 nonlinear constraints on the pure-component properties of the solvent are eliminated, such

982 as the feasibility of solvent storage and handling. In Test 2, the feasibility of achieving two  
983 phases at equilibrium at a specific stage of the separation unit is evaluated and an upper  
984 bound on feasible pressures is obtained. For each solvent that passes this test, the applica-  
985 tion of Test 3 provides an assessment of the feasibility of achieving the required purification  
986 of the feed and a lower bound on the feasible pressures. For each solvent that passes all  
987 tests, an initialization strategy is deployed prior to solution of the primal problem. This,  
988 combined with the updated bounds, reduces the likelihood of numerical failure during the  
989 solution of the primal. Finally, information from the tests and the solution of the primal  
990 problem is embedded in the master problem formulation to tighten the formulation and  
991 global convexity cuts are used to avoid including linearizations of the feasible region that  
992 are not valid underestimators of the non-convex feasible region in the master problem. The  
993 specific formulation of some of tests is developed with a focus on the design of absorption-  
994 desorption systems and three case studies on the design of a process for the separation of  
995 methane and carbon dioxide, given different specifications, are chosen to investigate the  
996 performance of the proposed approach. Different optimal solvents and process conditions  
997 are identified for each case study, confirming the strong interactions between solvent and  
998 process design.

999 A systematic investigation of the performance of the proposed algorithm is undertaken  
1000 by solving each case study from ten different starting points, using a fully automated  
1001 implementation. Convergence is successfully achieved in all thirty runs. The results show  
1002 that the tests offer several benefits in terms of increased robustness and computational  
1003 efficiency. The realization that a candidate solvent molecule is infeasible early on in a  
1004 major iteration eliminates the need to solve the primal problem at that iteration. Over  
1005 the thirty runs, only 8.1% of the solvent design space is probed. Thanks to the removal of  
1006 some solvents by the tests, evaluations of the primal problem is attempted for only 6.6% of  
1007 the solvent design space, highlighting the advantages of the proposed optimization-based  
1008 method over enumeration. Given that the solvent design space considered is relatively small

1009 and focused on classes of molecules that are known to offer good separation performance  
1010 for CO<sub>2</sub> and CH<sub>4</sub>,<sup>47</sup> the approach can be expected to be even more effective for larger  
1011 molecular design spaces.

1012 For feasible molecules, the tests help to remove infeasible regions from the search domain  
1013 and this can enhance convergence in a number of ways: some combinations of pressures  
1014 and temperatures which favour the incidence of discontinuities such as the appearance  
1015 and disappearance of phases in the absorber can be eliminated by using Test 0 and Test  
1016 2; optimizing over a reduced domain, thanks to Test 0, Test 2, or Test 3, may lead to a  
1017 smaller number of iterations of the nonlinear optimization solver, decreasing computational  
1018 cost; within the reduced domain, there is a reduced likelihood of encountering points where  
1019 the nature of phase behaviour (the number and type of phases) deviates from expected  
1020 behaviour; finally, initial guesses that are feasible from a thermodynamic perspective can  
1021 be identified more readily. Further, the tests, which carry only a small computational cost,  
1022 do not require the introduction of any further complexity into the process model itself,  
1023 and thus existing implementations of process models can be used directly in the proposed  
1024 algorithm.

1025 Due to its increased robustness, the proposed methodology makes it possible to tackle  
1026 highly nonlinear CAMPD problems without resorting to problem decomposition. This  
1027 moves the focus of CAMPD away from making simplifying assumptions that make the  
1028 problem tractable. In developing the process and thermophysical property models, em-  
1029 phasis can be placed instead on choosing the most appropriate model in terms of accuracy.  
1030 The increased robustness also makes it possible to adopt a strategy in which the non-convex  
1031 MINLP is solved from different starting points, increasing the likelihood of identifying the  
1032 global solution, a useful capability given that the use of deterministic global optimization  
1033 techniques is not yet feasible for problems of this size and complexity, characterized by  
1034 numerous highly nonlinear constraints. To the best of our knowledge, deterministic global  
1035 optimization techniques have not been currently applied to problems that include equilib-

1036 rium stage-based models of separation units with phase equilibrium described by rigorous  
1037 thermodynamic models.<sup>68</sup> The impact of non-convexities is clearly seen in one of the case  
1038 studies in which the algorithm converged to very different solutions from different starting  
1039 points.

1040 There is scope to apply the proposed modified outer approximation algorithm or tests  
1041 to increase solution robustness in a wide range of design problems. Given that the tests are  
1042 derived from a thermodynamic analysis of pure component and mixture behaviour, they can  
1043 readily be applied to solve property-based CAMD problems, where the process model is not  
1044 embedded within the optimization formulation. They can also be used to facilitate process  
1045 optimization even when the solvent molecule is fixed, by deploying Tests 0, 2, and 3 and  
1046 the initialization strategy prior to solving the full process optimization problem. A similar  
1047 test-based strategy may be applied to the design of other types of solvent-based separation  
1048 systems, such as liquid-liquid extraction systems, through appropriate modifications of the  
1049 proposed tests. For example, in the design of a liquid-liquid extraction system, the use of  
1050 a test similar to Test 2 might eliminate solvents that are fully miscible with the feed. In an  
1051 extractive distillation system, the use of a test based on Test 3 may allow for the screening  
1052 of process conditions and entrainers with which the required distillate composition may be  
1053 obtained. Finally, the set of tests can be expanded by incorporating additional implicit  
1054 and explicit process constraints, just as in our current work.

## 1055 **Acknowledgements**

1056 The authors gratefully acknowledge financial support from the Engineering and Physical  
1057 Sciences Research Council (EPSRC) grants EP/E016340, EP/J014958/1 and EP/J003840/1.  
1058 SG is grateful for an Imperial College PhD Scholarship.

## References

- 1059
- 1060 [1] Adjiman CS, Galindo A, Jackson G. Molecules matter: The expanding envelope of  
1061 process design. In: *Proceedings of the 8th International Conference on Foundations of*  
1062 *Computer-Aided Process Design*, edited by Eden MR, Siirola JD, Towler GP, vol. 34  
1063 of *Computer Aided Chemical Engineering*, pp. 55–64. Elsevier. 2014. Available online:  
1064 <http://www.sciencedirect.com/science/article/pii/B9780444634337500079>
- 1065 [2] Eden MR, Jørgensen SB, Gani R, El-Halwagi MM. A novel framework for simulta-  
1066 neous separation process and product design. *Chemical Engineering and Processing:*  
1067 *Process Intensification*. 2004;43:595–608.
- 1068 [3] Hostrup M, Harper PM, Gani R. Design of environmentally benign processes: in-  
1069 tegration of solvent design and separation process synthesis. *Computers & Chemical*  
1070 *Engineering*. 1999;23:1395–1414. Available online: [http://www.sciencedirect.com/](http://www.sciencedirect.com/science/article/pii/S0098135499003002)  
1071 [science/article/pii/S0098135499003002](http://www.sciencedirect.com/science/article/pii/S0098135499003002)
- 1072 [4] Pistikopoulos EN, Stefanis SK. Optimal solvent design for environmental impact min-  
1073 imization. *Computers & Chemical Engineering*. 1998;22(6):717–733. Available online:  
1074 <http://www.sciencedirect.com/science/article/pii/S009813549700255X>
- 1075 [5] Pereira FE, Keskes E, Galindo A, Jackson G, Adjiman CS. Integrated solvent and  
1076 process design using a SAFT-VR thermodynamic description: High-pressure sepa-  
1077 ration of carbon dioxide and methane. *Computers & Chemical Engineering*. 2011;  
1078 35:474–491.
- 1079 [6] Odele O, Macchietto S. Computer aided molecular design: a novel method for optimal  
1080 solvent selection. *Fluid Phase Equilibria*. 1993;82(0):47–54. Available online: [http://](http://www.sciencedirect.com/science/article/pii/037838129387127M)  
1081 [www.sciencedirect.com/science/article/pii/037838129387127M](http://www.sciencedirect.com/science/article/pii/037838129387127M)
- 1082 [7] Pretel EJ, Lopez PA, Bottini SB, Brignole EA. Computer-aided molecular design of

- 1083 solvents for separation processes. *AIChE Journal*. 1994;40(8):1349–1360. Available  
1084 online: <http://dx.doi.org/10.1002/aic.690400808>
- 1085 [8] Buxton A, Livingston AG, Pistikopoulos EN. Optimal design of solvent blends for  
1086 environmental impact minimization. *AIChE Journal*. 1999;45(4):817–843. Available  
1087 online: <http://dx.doi.org/10.1002/aic.690450415>
- 1088 [9] Struebing H, Ganase Z, Karamertzanis P, Sioukrou E, Haycock P, Piccione P, Arm-  
1089 strong A, Galindo A, Adjiman C. Computer-aided molecular design of solvents for  
1090 accelerated reaction kinetics. *Nature Chemistry*. 2013;5:952–957. Available online:  
1091 <http://dx.doi.org/10.1038/NCHEM.1755>
- 1092 [10] Apostolakou A, Adjiman CS. Chapter 4: Optimization methods in CAMD-II. In:  
1093 *Computer Aided Molecular Design: Theory and Practice*, edited by Achenie LE, Gani  
1094 R, Venkatasubramanian V, vol. 12 of *Computer Aided Chemical Engineering*, pp.  
1095 63–93. Elsevier. 2002. Available online: [http://www.sciencedirect.com/science/  
1096 article/pii/S1570794603800068](http://www.sciencedirect.com/science/article/pii/S1570794603800068)
- 1097 [11] Churi N, Achenie LEK. On the use of a mixed integer nonlinear programming model  
1098 for refrigerant design. *International Transactions of Operational Research*. 1997;4:45–  
1099 54.
- 1100 [12] Papadopoulos AI, Stijepovic M, Linke P, Seferlis P, Voutetakis S. Toward optimum  
1101 working fluid mixtures for organic rankine cycles using molecular design and sensitiv-  
1102 ity analysis. *Industrial & Engineering Chemistry Research*. 2013;52(34):12116–12133.  
1103 Available online: <http://dx.doi.org/10.1021/ie400968j>
- 1104 [13] Jonuzaj S, Akula PT, Kleniati PM, Adjiman CS. The formulation of optimal mixtures  
1105 with generalized disjunctive programming: A solvent design case study. *AIChE Jour-  
1106 nal*. 2016;pp. n/a–n/a. Available online: <http://dx.doi.org/10.1002/aic.15122>



- 1107 [14] Jonuzaj S, Adjiman CS. Designing optimal mixtures using generalized disjunctive  
1108 programming: Hull relaxations. manuscript submitted to. *Chem Eng Sci.* 2016;.
- 1109 [15] Fredenslund A, Jones RL, Prausnitz JM. Group-contribution estimation of activity  
1110 coefficients in nonideal liquid mixtures. *AIChE Journal.* 1975;21(6):1086–1099. Avail-  
1111 able online: <http://dx.doi.org/10.1002/aic.690210607>
- 1112 [16] Papaioannou V, Lafitte T, Avendaño C, Adjiman CS, Jackson G, Müller EA, Galindo  
1113 A. Group contribution methodology based on the statistical associating fluid theory for  
1114 heteronuclear molecules formed from Mie segments. *The Journal of Chemical Physics.*  
1115 2014;140(5):054107. Available online: [http://scitation.aip.org/content/aip/  
1116 journal/jcp/140/5/10.1063/1.4851455](http://scitation.aip.org/content/aip/journal/jcp/140/5/10.1063/1.4851455)
- 1117 [17] Majer C, Marquardt W, Gilles E. Reinitialization of dae’s after discontinuities. *Com-  
1118 puters & Chemical Engineering.* 1995;19, Supplement 1:507 – 512. Available online:  
1119 <http://www.sciencedirect.com/science/article/pii/0098135495870873>
- 1120 [18] Yeomans H, Grossmann IE. Disjunctive programming models for the optimal de-  
1121 sign of distillation columns and separation sequences. *Industrial & Engineering  
1122 Chemistry Research.* 2000;39(6):1637–1648. Available online: [http://dx.doi.org/  
1123 10.1021/ie9906520](http://dx.doi.org/10.1021/ie9906520)
- 1124 [19] Kamath RS, Biegler LT, Grossmann IE. An equation-oriented approach for handling  
1125 thermodynamics based on cubic equation of state in process optimization. *Computers  
1126 & Chemical Engineering.* 2010;34(12):2085–2096.
- 1127 [20] Skiborowski M, Harwardt A, Marquardt W. Efficient optimization-based design  
1128 for the separation of heterogeneous azeotropic mixtures. *Computers & Chemi-  
1129 cal Engineering.* 2015;72:34–51. Available online: [http://www.sciencedirect.com/  
1130 science/article/pii/S009813541400091X](http://www.sciencedirect.com/science/article/pii/S009813541400091X)

- 1131 [21] Eljack FT, Solvason CC, Chemmangattuvalappil N, Eden MR. A property based  
1132 approach for simultaneous process and molecular design. *Chinese Journal of Chemical*  
1133 *Engineering*. 2008;16:424–434.
- 1134 [22] Bommareddy S, Chemmangattuvalappil NG, Solvason CC, Eden MR. An  
1135 algebraic approach for simultaneous solution of process and molecular de-  
1136 sign problems. *Brazilian Journal of Chemical Engineering*. 2010;27:441–450.  
1137 Available online: [http://www.scielo.br/scielo.php?script=sci\\_arttext&pid=](http://www.scielo.br/scielo.php?script=sci_arttext&pid=S0104-66322010000300008&nrm=iso)  
1138 [S0104-66322010000300008&nrm=iso](http://www.scielo.br/scielo.php?script=sci_arttext&pid=S0104-66322010000300008&nrm=iso)
- 1139 [23] Chemmangattuvalappil NG, Eden MR. A novel methodology for property-based  
1140 molecular design using multiple topological indices. *Industrial & Engineering Chem-*  
1141 *istry Research*. 2013;52(22):7090–7103. Available online: [http://dx.doi.org/10.](http://dx.doi.org/10.1021/ie302516v)  
1142 [1021/ie302516v](http://dx.doi.org/10.1021/ie302516v)
- 1143 [24] Bardow A, Steur K, Gross J. Continuous-molecular targeting for integrated solvent  
1144 and process design. *Industrial & Engineering Chemistry Research*. 2010;49(6):2834–  
1145 2840. Available online: <http://dx.doi.org/10.1021/ie901281w>
- 1146 [25] Bardow A, Steur K, Gross J. A continuous targeting approach for integrated solvent  
1147 and process design based on molecular thermodynamic models. In: *10th Interna-*  
1148 *tional Symposium on Process Systems Engineering: Part A*, edited by Alves NC R,  
1149 Biscaia E EC, vol. 27 of *Computer Aided Chemical Engineering*, pp. 813–818. El-  
1150 sevier. 2009. Available online: [http://www.sciencedirect.com/science/article/](http://www.sciencedirect.com/science/article/pii/S1570794609703566)  
1151 [pii/S1570794609703566](http://www.sciencedirect.com/science/article/pii/S1570794609703566)
- 1152 [26] Gross J, Sadowski G. Perturbed-chain SAFT: an equation of state based on a per-  
1153 turbation theory for chain molecules. *Industrial & Engineering Chemistry Research*.  
1154 2001;40(4):1244–1260. Available online: <http://dx.doi.org/10.1021/ie0003887>

- 1155 [27] Lampe M, Gross J, Bardow A. Simultaneous process and working fluid  
1156 optimisation for organic rankine cycles (ORC) using PC-SAFT. *Com-*  
1157 *puter Aided Chemical Engineering*. 2012;30:572–576. Available online: [http:](http://www.scopus.com/inward/record.url?eid=2-s2.0-84862876235&partnerID=40&md5=1eedc4d95051e16895bb0e6da9111086)  
1158 [//www.scopus.com/inward/record.url?eid=2-s2.0-84862876235&partnerID=](http://www.scopus.com/inward/record.url?eid=2-s2.0-84862876235&partnerID=40&md5=1eedc4d95051e16895bb0e6da9111086)  
1159 [40&md5=1eedc4d95051e16895bb0e6da9111086](http://www.scopus.com/inward/record.url?eid=2-s2.0-84862876235&partnerID=40&md5=1eedc4d95051e16895bb0e6da9111086)
- 1160 [28] Lampe M, Stavrou M, Schilling J, Sauer E, Gross J, Bardow A. Computer-aided molec-  
1161 ular design in the continuous-molecular targeting framework using group-contribution  
1162 PC-SAFT. *Computers & Chemical Engineering*. 2015;81:278–287. Available online:  
1163 <http://www.sciencedirect.com/science/article/pii/S009813541500109X>
- 1164 [29] Karunanithi AT, Achenie LEK, Gani R. A new decomposition-based computer-aided  
1165 molecular/mixture design methodology for the design of optimal solvents and sol-  
1166 vent mixtures. *Industrial & Engineering Chemistry Research*. 2005;44(13):4785–4797.  
1167 Available online: <http://pubs.acs.org/doi/abs/10.1021/ie049328h>
- 1168 [30] Roughton BC, Christian B, White J, Camarda KV, Gani R. Simultaneous design of  
1169 ionic liquid entrainers and energy efficient azeotropic separation processes. *Com-*  
1170 *puters & Chemical Engineering*. 2012;42:248–262. Available online: [http://www.](http://www.sciencedirect.com/science/article/pii/S0098135412000774)  
1171 [sciencedirect.com/science/article/pii/S0098135412000774](http://www.sciencedirect.com/science/article/pii/S0098135412000774)
- 1172 [31] Kossack S, Kraemer K, Gani R, Marquardt W. A systematic synthesis framework  
1173 for extractive distillation processes. *Chemical Engineering Research and Design*.  
1174 2008;86(7):781–792. Available online: [http://www.sciencedirect.com/science/](http://www.sciencedirect.com/science/article/pii/S0263876208000257)  
1175 [article/pii/S0263876208000257](http://www.sciencedirect.com/science/article/pii/S0263876208000257)
- 1176 [32] Papadopoulos AI, Linke P. Multiobjective molecular design for integrated process-  
1177 solvent systems synthesis. *AIChE Journal*. 2006;52(3):1057–1070. Available online:  
1178 <http://dx.doi.org/10.1002/aic.10715>

- 1179 [33] Papadokonstantakis S, Badr S, Hungerbühler K, Papadopoulos AI, Damartzis T, Se-  
1180 ferlis P, Forte E, Chremos A, Galindo A, Jackson G, Adjiman CS. Chapter 11 - toward  
1181 sustainable solvent-based postcombustion CO<sub>2</sub> capture: From molecules to conceptual  
1182 flowsheet design. In: *Sustainability of Products, Processes and Supply Chains Theory  
1183 and Applications*, edited by You F, vol. 36 of *Computer Aided Chemical Engineering*,  
1184 pp. 279 – 310. Elsevier. 2015. Available online: [http://www.sciencedirect.com/  
1185 science/article/pii/B9780444634726000112](http://www.sciencedirect.com/science/article/pii/B9780444634726000112)
- 1186 [34] Papadopoulos AI, Linke P. Efficient integration of optimal solvent and process design  
1187 using molecular clustering. *Chemical Engineering Science*. 2006;61:6316–6336.
- 1188 [35] Papadopoulos A, Linke P. A unified framework for integrated process and molecular  
1189 design. *Chemical Engineering Research and Design*. 2005;83:674–678.
- 1190 [36] Papadopoulos AI, Seferlis P, Linke P. A framework for the integration of solvent  
1191 and process design with controllability assessment. *Chemical Engineering Science*.  
1192 2016;pp. –. Available online: [http://www.sciencedirect.com/science/article/  
1193 pii/S0009250916302135](http://www.sciencedirect.com/science/article/pii/S0009250916302135)
- 1194 [37] Zhou T, Zhou Y, Sundmacher K. A hybrid stochasticdeterministic optimization ap-  
1195 proach for integrated solvent and process design. *Chemical Engineering Science*. 2016;  
1196 pp. –. Available online: [http://www.sciencedirect.com/science/article/pii/  
1197 S0009250916301348](http://www.sciencedirect.com/science/article/pii/S0009250916301348)
- 1198 [38] Jaksland CA, Gani R, Lien KM. Separation process design and synthesis  
1199 based on thermodynamic insights. *Chemical Engineering Science*. 1995;50(3):511  
1200 – 530. Available online: [http://www.sciencedirect.com/science/article/pii/  
1201 000925099400216E](http://www.sciencedirect.com/science/article/pii/S000925099400216E)
- 1202 [39] Gil-Villegas A, Galindo A, Whitehead PJ, Mills SJ, Jackson G, Burgess AN. Statistical

- 1203 associating fluid theory for chain molecules with attractive potentials of variable range.  
1204 *The Journal of Chemical Physics*. 1997;106:4168–4186.
- 1205 [40] Galindo A, Davies LA, Gil-Villegas A, Jackson G. The thermodynamics of mixtures  
1206 and the corresponding mixing rules in the SAFT-VR approach for potentials of vari-  
1207 able range. *Molecular Physics*. 1998;93:241–252.
- 1208 [41] Zhou T, McBride K, Zhang X, Qi Z, Sundmacher K. Integrated solvent and process  
1209 design exemplified for a Diels-Alder reaction. *AIChE Journal*. 2015;61(1):147–158.  
1210 Available online: <http://dx.doi.org/10.1002/aic.14630>
- 1211 [42] Cheng HC, Wang FS. Computer-aided biocompatible solvent design for an inte-  
1212 grated extractive fermentation-separation process. *Chemical Engineering Journal*.  
1213 2010;162(2):809 – 820. Available online: [http://www.sciencedirect.com/science/  
1214 article/pii/S1385894710005413](http://www.sciencedirect.com/science/article/pii/S1385894710005413)
- 1215 [43] Exler O, Schittkowski K. A trust region sqp algorithm for mixed-integer nonlinear  
1216 programming. *Optimization Letters*. 2007;1(3):269–280. Available online: [http:  
1217 //www.scopus.com/inward/record.url?eid=2-s2.0-34249017940&partnerID=  
1218 40&md5=ac8730f8f908cf80762413db758135be](http://www.scopus.com/inward/record.url?eid=2-s2.0-34249017940&partnerID=40&md5=ac8730f8f908cf80762413db758135be)
- 1219 [44] Schilling J, Lampe M, Gross J, Bardow A. 1-stage CoMT-CAMD: An approach  
1220 for integrated design of {ORC} process and working fluid using pc-saft. *Chemical  
1221 Engineering Science*. 2016;pp. –. Available online: [http://www.sciencedirect.com/  
1222 science/article/pii/S0009250916302196](http://www.sciencedirect.com/science/article/pii/S0009250916302196)
- 1223 [45] Geoffrion A. Generalized Benders decomposition. *Journal of Optimization Theory and  
1224 Applications*. 1972;10(4):237–260. Available online: [http://dx.doi.org/10.1007/  
1225 BF00934810](http://dx.doi.org/10.1007/BF00934810)
- 1226 [46] Giovanoglou A, Barlatier J, Adjiman CS, Pistikopoulos EN, Cordiner JL. Optimal

- 1227 solvent design for batch separation based on economic performance. *AIChE Jour-*  
1228 *nal.* 2003;49(12):3095–3109. Available online: [http://dx.doi.org/10.1002/aic.](http://dx.doi.org/10.1002/aic.690491211)  
1229 690491211
- 1230 [47] Burger J, Papaioannou V, Gopinath S, Jackson G, Galindo A, Adjiman CS. A hier-  
1231 archical method to integrated solvent and process design of physical CO<sub>2</sub> absorption  
1232 using the SAFT- $\gamma$  Mie approach. *AIChE Journal.* 2015;61:3249–3269. Available on-  
1233 line: <http://dx.doi.org/10.1002/aic.14838>
- 1234 [48] Gopinath S, Galindo A, Jackson G, Adjiman CS. A feasibility-based algorithm for  
1235 computer aided molecular and process design of solvent-based separation systems. In:  
1236 *Proceedings of the 26th European Symposium on Computer Aided Process Engineering,*  
1237 edited by Kravanja Z, Computer Aided Chemical Engineering. Elsevier B.V. 2016.
- 1238 [49] Duran MA, Grossmann IE. An outer-approximation algorithm for a class of mixed-  
1239 integer nonlinear programs. *Mathematical Programming.* 1986;36(3):307–339. Avail-  
1240 able online: <http://dx.doi.org/10.1007/BF02592064>
- 1241 [50] Fletcher R, Leyffer S. Solving mixed integer nonlinear programs by outer ap-  
1242 proximation. *Mathematical Programming.* 1994;66(1-3):327–349. Available online:  
1243 <http://dx.doi.org/10.1007/BF01581153>
- 1244 [51] Chapman WG, Gubbins KE, Jackson G, Radosz M. New reference equation of state  
1245 for associating liquids. *Industrial & Engineering Chemistry Research.* 1990;29:1709–  
1246 1721.
- 1247 [52] Chapman WG, Gubbins KE, Jackson G, Radosz M. SAFT: Equation-of-state solution  
1248 model for associating fluids. *Fluid Phase Equilibria.* 1989;52:31–38.
- 1249 [53] McCabe C, Galindo A. Chapter 8 saft associating fluids and fluid mixtures. In:

- 1250 *Applied Thermodynamics of Fluids*, pp. 215–279. The Royal Society of Chemistry.  
1251 2010. Available online: <http://dx.doi.org/10.1039/9781849730983-00215>
- 1252 [54] Kontogeorgis GM, Folas GK. *Thermodynamic Models for Industrial Applications:*  
1253 *From Classical and Advanced Mixing Rules to Association Theories*. John Wiley &  
1254 Sons: New York. 2010.
- 1255 [55] Conte E, Martinho A, Matos HA, Gani R. Combined group-contribution and atom  
1256 connectivity index-based methods for estimation of surface tension and viscosity. *In-*  
1257 *dustrial & Engineering Chemistry Research*. 2008;47(20):7940–7954. Available online:  
1258 <http://pubs.acs.org/doi/abs/10.1021/ie071572w>
- 1259 [56] Sastri S, Rao K. A new group contribution method for predicting viscosity of organic  
1260 liquids. *The Chemical Engineering Journal*. 1992;50:9–25. Available online: <http://www.sciencedirect.com/science/article/pii/030094679280002R>  
1261
- 1262 [57] Macleod DB. On a relation between surface tension and density. *Trans Faraday Soc*.  
1263 1923;19:38–41. Available online: <http://dx.doi.org/10.1039/TF9231900038>
- 1264 [58] Process Systems Enterprise. gPROMS. 1997-2015. Available online: [www.psenderprise.com/gproms](http://www.psenderprise.com/gproms)  
1265  
1266
- 1267 [59] Harper PM, Gani R, Kolar P, Ishikawa T. Computer-aided molecular design  
1268 with combined molecular modeling and group contribution. *Fluid Phase Equi-*  
1269 *libria*. 1999;158160(0):337–347. Available online: <http://www.sciencedirect.com/science/article/pii/S0378381299000898>  
1270
- 1271 [60] Hunter TG, Nash AW. The application of physico-chemical principles to the design of  
1272 liquid-liquid contact equipment. Part II. Application of phase-rule graphical methods.  
1273 *Journal of the Society of Chemical Industry*. 1934;

- 1274 [61] Henley EJ, Seader JD, Roper DK. *Separation process principles, Third Edition, In-*  
1275 *ternational student version*. John Wiley & Sons (Asia) Pte Ltd. 2011.
- 1276 [62] Kravanja Z, Grossmann IE. New developments and capabilities in PROSYN-an au-  
1277 tomated topology and parameter process synthesizer. *Computers & Chemical En-*  
1278 *gineering*. 1994;18(1112):1097–1114. Available online: [http://www.sciencedirect.](http://www.sciencedirect.com/science/article/pii/S0098135494850275)  
1279 [com/science/article/pii/S0098135494850275](http://www.sciencedirect.com/science/article/pii/S0098135494850275)
- 1280 [63] Samudra AP, Sahinidis NV. Optimization-based framework for computer-aided molec-  
1281 ular design. *AIChE Journal*. 2013;59:3686–3701.
- 1282 [64] Gurobi Optimization, Inc. Gurobi optimizer reference manual. 2015. Available online:  
1283 <http://www.gurobi.com>
- 1284
- 1285 [65] Tan L, Shariff A, Lau K, Bustam M. Impact of high pressure on high concentration car-  
1286 bon dioxide capture from natural gas by monoethanolamine/n-methyl-2-pyrrolidone  
1287 solvent in absorption packed column. *International Journal of Greenhouse Gas Con-*  
1288 *trol*. 2015;34:25 – 30. Available online: [http://www.sciencedirect.com/science/](http://www.sciencedirect.com/science/article/pii/S1750583615000043)  
1289 [article/pii/S1750583615000043](http://www.sciencedirect.com/science/article/pii/S1750583615000043)
- 1290 [66] Baojia H, Xusheng L, Xianming X. Origin and accumulation of CO<sub>2</sub> in natural gases  
1291 of the Yinggehai-Qiongdongnan basins, offshore South China Sea. In: *Natural gas*  
1292 *geochemistry: Recent developments, applications, and technologies*. 2011.
- 1293 [67] Pereira FE, Jackson G, Galindo A, Adjiman CS. The HELD algorithm for mul-  
1294 ticomponent, multiphase equilibrium calculations with generic equations of state.  
1295 *Computers & Chemical Engineering*. 2012;36(0):99–118. Available online: [http:](http://www.sciencedirect.com/science/article/pii/S0098135411002365)  
1296 [//www.sciencedirect.com/science/article/pii/S0098135411002365">//www.sciencedirect.com/science/article/pii/S0098135411002365](http://www.sciencedirect.com/science/article/pii/S0098135411002365)
- 1297 [68] Skiborowski M, Rautenberg M, Marquardt W. A hybrid evolutionary-deterministic



1298 optimization approach for conceptual design. *Industrial & Engineering Chemistry*  
1299 *Research*. 2015;54(41):10054–10072. Available online: <http://dx.doi.org/10.1021/>  
1300 [acs.iecr.5b01995](http://dx.doi.org/10.1021/acs.iecr.5b01995)

## 1301 Appendix A

1302 Pressure can affect fluid-phase behaviour in different ways depending on the mixture under  
1303 consideration. In order to illustrate different situations, and given assumption 2, four types  
1304 of ternary phase diagrams that may be observed are sketched in Figure 6, at fixed pressure  
1305 and temperature, illustrating instances in which different pairs of compounds are partially  
1306 miscible. In Figure 6a, only the solvent-product binary mixture exhibits vapour-liquid  
1307 equilibrium (as in Figure 3); in Figure 6b, only the solvent-solute pair exhibits phase  
1308 separation; in Figure 6c, the two binary pairs of solvent-solute and solvent-product exhibit  
1309 vapour-liquid equilibrium; finally, in Figure 6d, the two binary pairs of product-solute and  
1310 product-solvent are partially miscible.

1311 For a mixture at conditions  $P$ ,  $T_N$  that exhibits behaviour of the types shown in Fig-  
1312 ures 3 and 6a, a further increase in pressure will result in a decrease in the size of the  
1313 vapour-liquid region. Thus, for systems that exhibit full miscibility of the solvent and the  
1314 solute the necessary condition identified above may be used to find the maximum feasible  
1315 value of pressure. Consider a mixture that exhibits partial miscibility of the solute-solvent  
1316 pair and full miscibility of the product-solvent pair (cf Figure 6b). At some pressure  
1317  $P' < P$ , the vapour-liquid envelope at  $P'$ , shown by the dashed curve in Figure 6b, results  
1318 in a vapour leaving stage  $N$  that has a lower concentration of product than the feed. Hence,  
1319 the operation of the stage at  $P'$  is infeasible with respect to achieving separation in the  
1320 desired direction. As  $\overline{\mathbf{y}_F \mathbf{x}_s}$  does not intersect the curve at conditions  $P'$ ,  $T_N$ , the necessary  
1321 condition derived here is not satisfied at  $P'$ , but is satisfied at some feasible pressure  $P$ ,  
1322 where  $P' > P$ . Thus, the application of the test to systems of the type shown in Figure 6b

1323 can also yield a maximum pressure beyond which separation is infeasible. Next, consider  
 1324 mixtures that exhibit partial miscibility of the solvent-solute and the solvent-product pairs  
 1325 (cf Figure 6c) at all pressures and temperatures within the process domain. The line  $\overline{\mathbf{y}_F \mathbf{x}_s}$   
 1326 intersects the two-phase region at any conditions  $P, T_N$ . Thus, since these mixtures satisfy  
 1327 the necessary condition identified, all pressures up to the user-defined upper bound are  
 1328 found to be feasible. Similarly, for systems that exhibit partial product-solute miscibility,  
 1329 as in Figure 6d, if line  $\overline{\mathbf{y}_F \mathbf{x}_s}$  intersects the two-phase region at  $P, T_N$ , pressure  $P$  is fea-  
 1330 sible. For mixtures for which the size of the two-phase region increases with pressure, the  
 1331 necessary condition of Test 2 may yield a maximum feasible pressure at or above the user-  
 1332 defined upper bound on allowable pressures, offering no improvement over the user-defined  
 1333 bound. Although ternary mixtures may exhibit more than one type of phase diagram as  
 1334 the conditions of pressure and temperature are varied, the necessary condition for Test 2  
 1335 is valid for each of type of ternary diagram and therefore across different conditions.

## 1336 Appendix B

1337 To reformulate Problem (P2), the objective function is multiplied  $\tanh(\beta(\|\mathbf{y}_N - \mathbf{x}_N\|_2$   
 1338  $-\epsilon))$ . Here,  $\beta$  is a positive scaling factor to ensure that the tanh function yields values very  
 1339 close to unity when its argument is positive. When the third constraint in (P2), which  
 1340 ensures that two distinct phases are obtained, is violated, the following holds:

$$\|\mathbf{y}_N - \mathbf{x}_N\|_2 - \epsilon < 0,$$

1341 and the objective function is thus multiplied by a negative number. This ensures that no  
 1342 increasing direction for the objective function is found when no two-phase solution is found.  
 1343 Thus, the solver converges to a solution in the neighbourhood of  $P_N^{U(k)}$ . The formulation

1344 is given by:

$$\begin{aligned}
P_N^{U(k)} = & \max_{P_N, T_N, \mathbf{y}_N, \mathbf{x}_N} && P_N \tanh(\beta(\|\mathbf{y}_N - \mathbf{x}_N\|_2 - \epsilon)) \\
\text{s.t.} & && \frac{y_{F,1} - x_{N,1}}{y_{F,2} - x_{N,2}} = \frac{y_{F,1} - x_{s,1}}{y_{F,2} - x_{s,2}} \\
& && \mu_i^V(\mathbf{y}_N, T_N, P_N, \mathbf{n}^{(k)}) = \mu_i^L(\mathbf{x}_N, T_N, P_N, \mathbf{n}^{(k)}) \quad \forall i = 1, \dots, NC \\
& && \sum_{i=1}^{NC} x_{N,i} = 1 \\
& && \sum_{i=1}^{NC} y_{N,i} = 1 \\
& && \|\mathbf{y}_N - \mathbf{x}_N\|_2 \geq \epsilon \\
& && P_{N+1}^L - PD \leq P_N \leq P_{N+1}^U \\
& && \max(T_{mp}(\mathbf{n}^{(k)}) + 10, T_N^L) \leq T_N \leq \min(T_F + 20, T_N^U) \\
& && 0 \leq \mathbf{x}_N \leq 1 \\
& && 0 \leq \mathbf{y}_N \leq 1
\end{aligned} \tag{P2a}$$

## 1345 Appendix C

1346 In order to solve for phase equilibrium more robustly for Test 3, the TPFlash routine in  
1347 gSAFT, an isothermal-isobaric flash routine, is used. The routine yields compositions and  
1348 thermodynamic properties of up to three phases in equilibrium, denoted by mole fractions  
1349  $\mathbf{y}$ ,  $\mathbf{xa}$ , and  $\mathbf{xb}$ . If a phase does not exist, the corresponding compositions are set equal to  
1350 zero in the output of this flash routine. Two phases in equilibrium may either be ordered  
1351 as  $\mathbf{y}$  and  $\mathbf{xa}$ , or as  $\mathbf{xa}$  and  $\mathbf{xb}$  in the output of the flash routine.

1352 In the input to the flash routine we used an overall composition of  $\mathbf{z}$ , chosen to be a point  
1353 very close to the product-solvent boundary. An overall composition on that boundary, such  
1354 that  $z_1$  is smaller than  $y_p$ , is one most likely to result in an equilibrium composition of the  
1355 vapour phase that is rich in the product.  $z_1$  was set at 0.9 in this study, where the required  
1356 purity  $y_p$  ranges from 0.97 to 0.99 assuming the liquid boundary has compositions of the

1357 product lower than  $z_1$ . Hence, if two-phases exist at  $y_p$  or greater, the overall composition  $\mathbf{z}$   
 1358 will split into two. Alternatively,  $z_1$  could be set equal to  $y_p$ , thus requiring no assumption  
 1359 on the liquid boundary.

$$\begin{aligned}
 P_1^{L(k)} &= \min_{P_1, T_1} P_1 \\
 \text{s.t.} \quad \mathbf{z} &= [0.9 \quad \epsilon \quad 0.1 - \epsilon]^T \\
 [\mathbf{y} \quad \mathbf{x}\mathbf{a} \quad \mathbf{x}\mathbf{b}]^T &= \text{TPFlash}(\mathbf{z}, T_1, P_1, \mathbf{n}^{(k)}) \\
 \max(y_1, xa_1, xb_1) &> y_p \\
 \|\mathbf{y} - \mathbf{x}\mathbf{a}\|_2 &> \epsilon \\
 \|\mathbf{x}\mathbf{a} - \mathbf{x}\mathbf{b}\|_2 &> \epsilon \\
 P_1^L &\leq P_1 \leq P_1^U \\
 \max(T_{mp}(\mathbf{n}^{(k)}) + 10, T_1^L) &\leq T_1 \leq \min(T_F + 20, T_1^U)
 \end{aligned} \tag{P3a}$$

## 1360 Appendix D

1361 The following steps are taken to overcome numerical issues arising from the nonlinearity  
 1362 and non-convexity of Problems (P2), (P3) and (P4):

1363 (i) The robust algorithm for constant pressure and temperature flash calculations im-  
 1364 plemented within gPROMS is used in Test 3 instead of including the necessary con-  
 1365 ditions for phase equilibrium as part of the model equations. Note that while the  
 1366 flash equation was used in (P3a), it was not used in (P2a) or (P4). In the gPROMS  
 1367 modelling platform, which follows a feasible path approach with respect to equality  
 1368 constraints, a variable is either a degree of freedom (or input) or its value is obtained  
 1369 by the solution of a system of equations. The flash equations require temperature,  
 1370 pressure and total composition as inputs. In Test 3, all of the inputs to the flash  
 1371 methods are degrees of freedom, hence it is straightforward to use the flash algorithm  
 1372 to solve for phase equilibrium. However, in an initial analysis, the use of the flash  
 1373 algorithm seemed to make the solution of problems (P4) and (P2a) less robust as

1374 in these the temperature and composition variables, respectively, are not degrees of  
 1375 freedom.

1376 (ii) Starting points that are likely to be feasible for the two tests and Problem (P4) are  
 1377 generated at each iteration. For Test 2, the initial guess of pressure is set at  $P_N^L$ ,  
 1378 a pressure which is most likely to be feasible. The initial guess of temperature is  
 1379 set as  $\min(T_F + 20, T_N^U)$ . A flash problem is then solved for a mixture with total  
 1380 composition equal to the arithmetic mean of the feed and pure solvent compositions  
 1381 and at the initial guess of pressure and temperature. The equilibrium compositions,  
 1382 if they exist, are then used to initialize problem (P2). For Test 3, the initial guess  
 1383 of  $T_1$  is set at its lower bound as it is most likely to be feasible. The pressure on  
 1384 the other hand, is set at its upper bound. For Problem (P4), given a known solution  
 1385  $(\mathbf{u}_0, \mathbf{n}_0, \mathbf{x}_0^d)$  to the model equations, an initial guess for  $\mathbf{x}^d$  at iteration  $k$ , where the  
 1386 solvent is given by  $\mathbf{n}^{(k)}$ , is obtained by solving the following problem:

$$\begin{aligned}
 \mathbf{h}(\mathbf{n}(t), \mathbf{x}^d(t), \mathbf{u}_0) &= 0 \\
 \frac{d\mathbf{n}(t)}{dt} &= 0.001(\mathbf{n}^{(k)} - \mathbf{n}_0) \\
 \mathbf{n}(0) &= \mathbf{n}_0 \\
 \mathbf{n}(t = 1000) &= \mathbf{n}^{(k)},
 \end{aligned}
 \tag{P4I}$$

1387 so that  $(\mathbf{u}_0, \mathbf{n}^{(k)}, \mathbf{x}^d(t = 1000))$  can be used as an initial guess for (P4). Problem (P4I)  
 1388 is a differential-algebraic system of equations in which initial and final conditions on  
 1389 the solvent structure are specified. Such a problem can be solved provided that the  
 1390 physical property models allow the solvent structure to be set with a real-valued input  
 1391 for the number of groups of a given type. Thus, provided that one feasible point is  
 1392 known for the primal problem, it can often be used to derive initial guesses for the  
 1393 solution of other primal problems. Problem (P4I) is implemented in gPROMS, as  
 1394 the other primal subproblems.

1395 (iii) The infeasibility of Problems (P2a) and (P3a) is handled in different ways depending  
1396 on the root cause: in gPROMS, a problem is reported to be infeasible if either no  
1397 solution to the model equations (equality constraints) is found at the starting guess,  
1398 that is the equality constraints cannot be initialized at the initial guess, or if no  
1399 solution is found that satisfies both the equality and inequality constraints, that  
1400 is the solver generates points where the equality constraints are satisfied but the  
1401 inequality constraints are violated. If the first case occurs, in this algorithm, the test  
1402 is treated as inconclusive in the CAMPD algorithm, as a failure to initialize model  
1403 equations, whereas in the latter case the test is treated as infeasible.

1404

1405 The values assigned to the constants that appear in the formulations (P2a), (P3a) and (M)  
1406 are shown in Table 10.

1407 **List of Tables**

1408	1	Procedure for Test 0. . . . .	64
1409	2	Variable bounds common to all case studies. . . . .	65
1410	3	Specifications that vary depending on the case study. . . . .	66
1411	4	Initial guesses used to solve problems C1, C2, C3. . . . .	67
1412	5	Effectiveness of Tests 1, 2 and 3 over all 109 solvents, for the specifications	
1413		of each of the case studies. . . . .	68
1414	6	Locally optimal solution for each case study from ten different starting	
1415		points. The * superscript denotes locally optimal solutions. . . . .	69
1416	7	Performance of the algorithm and tests for case studies C1, C2 and C3,	
1417		based on aggregate values over the ten starting points for each case study.	
1418		The percentages of iterations over which a given test is active are calculated	
1419		based on the total number of major iterations for the ten runs for the relevant	
1420		case study. . . . .	70
1421	8	Outcome of Test 0 for three different feed conditions ( $\text{CO}_2$ mole fraction,	
1422		$y_{\text{FCO}_2}$ , feed temperature, $T_F$ , feed pressure, $P_F$ ). The cricondentherm, $T_c$ ,	
1423		and updated pressure bound, $P_{abs}^{L0}$ , after Test 0 are reported. . . . .	71
1424	9	Detailed outcome of the proposed algorithm for the third iteration of the	
1425		solution of case study C2, using initial guess ID 4 as a starting point. The	
1426		solvent candidate is $n_{\text{CH}_3}^{(3)} = 2$ , $n_{\text{CH}_2}^{(3)} = 2$ , $n_{\text{eO}}^{(3)} = 2$ , $n_{\text{cO}}^{(3)} = 1$ . . . . .	72
1427	10	Values assigned to constants in the Problems (P2a), (P3a) and (M). . . . .	73

Table 1: Procedure for Test 0.

1. Calculate  $T_{cr}$  at composition  $\mathbf{y}_F$ .
2. Calculate  $T_{N+1}^{L0}$  using Eq. (1).
3. Calculate  $P_H$  using Eq. (2).
4. Calculate  $P_{N+1}^{L0}$  using Eq. (3).
5. Set  $T_{N+1}^L = T_{N+1}^{L0}$  and  $P_{N+1}^L = P_{N+1}^{L0}$ .



Table 2: Variable bounds common to all case studies.

Variable	Description	Units	Lower bound	Upper bound
$n_{\text{CH}_3}$	Number of $\text{CH}_2$ groups	–	2	2
$n_{\text{CH}_2}$	Number of $\text{CH}_2$ groups	–	0	8
$n_{\text{cO}}$	Number of cO groups	–	0	7
$n_{\text{eO}}$	Number of eO groups	–	0	2
$L_0$	Solvent flowrate entering absorber	$\text{kmol s}^{-1}$	0.01	50
$V_{N+1}$	Feed flowrate entering absorber	$\text{kmol s}^{-1}$	1	1
$P_{\text{abs}}$	Absorber pressure	MPa	0.1	Variable, cf. Table 3
$P_{\text{flash}}$	Pressure in the flash drum	MPa	0.1	0.1
$P_{\text{amb}}$	Pressure at the pure solvent inlet	MPa	0.1	0.1
$T_{N+1}$	Temperature of gas stream entering absorber	K	230	Feed temperature, $T_F$
$T_N$	Temperature on stage $N$	K	230	Variable, cf. Table 3
$T_1$	Temperature on stage 1	K	Variable, cf. Table 3	$T_F + 20$
$T_{sh}$	Solvent handling temperature	K	298	308
$T_s$	Temperature of the solvent feed to the absorber	K	298	298
$\nu$	Solvent viscosity at standard pressure and $T_s^L$	Pa s	0	0.1

Table 3: Specifications that vary depending on the case study.

Case Study	$y_{F_{CO_2}}$	$T_F/K$	$P_F/MPa$	$y_p$	$P_{abs}^U$	Valve	Extra constraint	$T_N^U/K$	$T_1^L/K$
C1	0.20	301.48	7.961	0.97	7.500	Yes	No	400	230
C2	0.92	340.00	$P_F = P_{abs}$	0.97	12.900	No	$T_N \leq T_N^U$	325	230
C3	0.50	325.00	9.800	0.99	9.800	Yes	$T_1 \geq T_1^L$	400	298

Table 4: Initial guesses used to solve problems C1, C2, C3.

Initial guess ID	$n_{\text{CH}_3}^0$	$n_{\text{CH}_2}^0$	$n_{\text{eO}}^0$	$n_{\text{cO}}^0$	$L_0^0$ kmols <sup>-1</sup>	$P_{abs}^0$ MPa
1	2	4	2	3	0.619	7.5
2	2	5	2	4	0.619	7.5
3	2	3	2	2	0.619	7.5
4	2	8	2	4	0.619	7.5
5	2	2	2	1	0.619	7.5
6	2	1	2	0	0.619	7.5
7	2	2	1	0	0.619	7.5
8	2	7	2	2	0.619	7.5
9	2	8	0	0	0.619	7.5
10	2	0	0	0	0.619	7.5

Table 5: Effectiveness of Tests 1, 2 and 3 over all 109 solvents, for the specifications of each of the case studies.

	Test 1	Test 2	Test 3
<hr/> <hr/> Case study C1 <hr/>			
Number of molecules tested	109	88	88
Number of molecules eliminated by test	21	0	0
Arithmetic mean of updated bound on pressure (MPa)	N/A	-	-
Number of molecules for which the test is active	21	0	0
<hr/> Case study C2 <hr/>			
Number of molecules tested	109	88	88
Number of molecules eliminated by test	21	0	0
Arithmetic mean of updated bound on pressure (MPa)	N/A	11.45	-
Number of molecules for which the test is active	21	18	0
<hr/> Case study C3 <hr/>			
Number of molecules tested	109	88	88
Number of molecules eliminated by test	21	0	1
Arithmetic mean of updated bound on pressure (MPa)	N/A	-	0.32
Number of molecules for which the test is active	21	0	10

Table 6: Locally optimal solution for each case study from ten different starting points. The \* superscript denotes locally optimal solutions.

Initial guess ID	$n_{\text{CH}_3}^*$	$n_{\text{CH}_2}^*$	$n_{\text{eO}}^*$	$n_{\text{cO}}^*$	$L_0^*/\text{kmol s}^{-1}$	$P_{\text{abs}}^*/\text{MPa}$	$NPV/10^9\text{USD}$
Case C1							
1-10	2	5	2	4	0.846	3.832	1.724
Case C2							
4	2	8	2	1	0.339	9.695	0.040
2,5,6,7,9,10	2	8	2	0	0.304	10.035	0.037
8	2	8	0	3	0.248	10.482	0.035
1	2	6	0	4	0.233	11.177	0.015
3	2	8	1	0	0.337	9.669	0.014
Case C3							
1-10	2	7	2	6	1.457	9.8	0.329

Table 7: Performance of the algorithm and tests for case studies C1, C2 and C3, based on aggregate values over the ten starting points for each case study. The percentages of iterations over which a given test is active are calculated based on the total number of major iterations for the ten runs for the relevant case study.

	C1	C2	C3
Arithmetic mean of the number of major iterations	11.8	10.6	4.7
Smallest number of major iterations	4	4	3
Largest number of major iterations	17	15	7
Standard deviation of the number of major iterations	5.5	4.6	1.1
Test 0 active	No	No	No
Percentage of iterations with Test 1 active	14.4	14.1	29.8
Percentage of iterations with Test 2 active	0.0	11.1	0.0
Percentage of iterations with Test 3 active	0.0	0.0	6.4
Arithmetic mean of the number of attempted primal evaluations	10.1	8.5	3.1

Table 8: Outcome of Test 0 for three different feed conditions (CO<sub>2</sub> mole fraction,  $y_{\text{CO}_2}$ , feed temperature,  $T_F$ , feed pressure,  $P_F$ ). The cricondentherm,  $T_c$ , and updated pressure bound,  $P_{abs}^{L0}$ , after Test 0 are reported.

Feed conditions			Test 0 outcome	
$y_{\text{CO}_2}$	$T_F/\text{K}$	$P_F/\text{MPa}$	$T_c/\text{K}$	$P_{abs}^{L0}/\text{MPa}$
0.30	290	12.000	237	3.637
0.50	301	10.000	260	4.312
0.80	301	8.000	288	6.532

Table 9: Detailed outcome of the proposed algorithm for the third iteration of the solution of case study C2, using initial guess ID 4 as a starting point. The solvent candidate is  $n_{\text{CH}_3}^{(3)} = 2$ ,  $n_{\text{CH}_2}^{(3)} = 2$ ,  $n_{\text{eO}}^{(3)} = 2$ ,  $n_{\text{cO}}^{(3)} = 1$ .

Problem	Status	Updated bound
Test 0	No update	–
Test 1	Passed	–
Test 2	Feasible	$P_{abs}^{U(2)} = 12.06490$ MPa
Test 3	Feasible	$P_{abs}^{L(2)} = 0.100095$ MPa
Primal	Process model: feasible Design constraints: infeasible	–



Table 10: Values assigned to constants in the Problems (P2a), (P3a) and (M).

Constant	Value
$\epsilon$	$10^{-3}$
$\epsilon_c$	$-10^{-3}$
$\epsilon_c$	9
$\epsilon_n$	$10^{-3}$
$\beta$	$10^4$
$b$	9
$M^L$	-7372
$M^U$	7372

1428 **List of Figures**

1429 1 A flowsheet for the removal of carbon dioxide from a natural gas stream via  
1430 absorption, as considered in Burger et al.<sup>47</sup> . . . . . 76

1431 2 A diagram illustrating isenthalpic expansion for a mixture of methane and  
1432 CO<sub>2</sub> with a constant total mole fraction of CO<sub>2</sub> of  $y_{FCO_2} = 0.8$ . The arrow  
1433 denotes the cricondentherm,  $T_{cr}$ . The thick solid curve denotes the dew  
1434 pressure as a function of temperature, as calculated using the SAFT- $\gamma$  Mie  
1435 equation of state<sup>47</sup>. Isenthalpic curves (thin solid curves) denote adiabatic  
1436 expansions from three points Ai, i=1,2,3 to three points Bi, i=1,2,3. . . . . 77

1437 3 A phase diagram for CO<sub>2</sub>-methane-solvent (propyl-methyl ether) at  $T_N =$   
1438 304.4 K,  $P_{abs} = 9.0$  MPa, illustrating the locus of difference points (dashed  
1439 lines, points  $\mathbf{d}'$ ,  $\mathbf{d}''$ ,  $\mathbf{o}'$  and  $\mathbf{o}''$ ) and infeasible operating lines as discussed  
1440 in the text.  $\mathbf{y}_1$  is the composition of the gas stream leaving the absorber,  
1441  $\mathbf{y}_F$  the composition of the feed stream entering the absorber and  $\mathbf{x}_s$  the  
1442 composition of the pure solvent stream entering the absorber. . . . . 78

1443 4 Phase diagram for CO<sub>2</sub>-methane-solvent (propyl-methyl ether) at  $T_1 = 270$   
1444 K and pressure  $P_1$ . a)  $P_1 = 0.1$  MPa. b)  $P_1 = 0.610$  MPa. The shaded  
1445 region represents  $y_{1,1} \geq y_p = 0.97$  . . . . . 79

1446 5 A flowchart of the proposed algorithm. . . . . 80

1447 6 Four types of ternary phase diagrams for a product (1), solute (2) and solvent  
 1448 (3) at constant pressure and temperature. a) The solvent and product pair  
 1449 is partially miscible and other pairs are fully miscible; b) The solvent and  
 1450 solute pair is partially miscible and other pairs are fully miscible; c) The  
 1451 solvent and solute pair is partially miscible and the solvent and product  
 1452 pair is partially miscible; d) The product and solute pair is partially miscible  
 1453 and the solvent and product pair is partially miscible.  $\mathbf{y}_F$  denotes the feed  
 1454 composition,  $\mathbf{y}_1$  denotes the product composition and  $\mathbf{x}_s$  the lean solvent  
 1455 composition. The thick curves denote the vapour-liquid envelope at pressure  
 1456  $P$ . The dashed curves indicate the vapour-liquid envelope at a pressure  $P'$ ,  
 1457 such that  $P > P'$ . . . . . 81

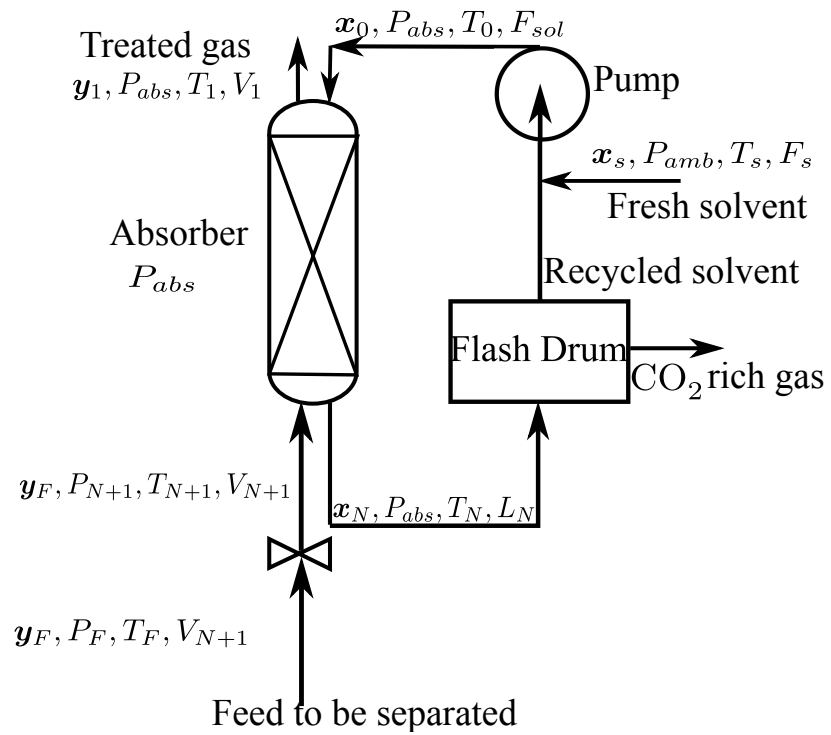


Figure 1: A flowsheet for the removal of carbon dioxide from a natural gas stream via absorption, as considered in Burger et al.<sup>47</sup>

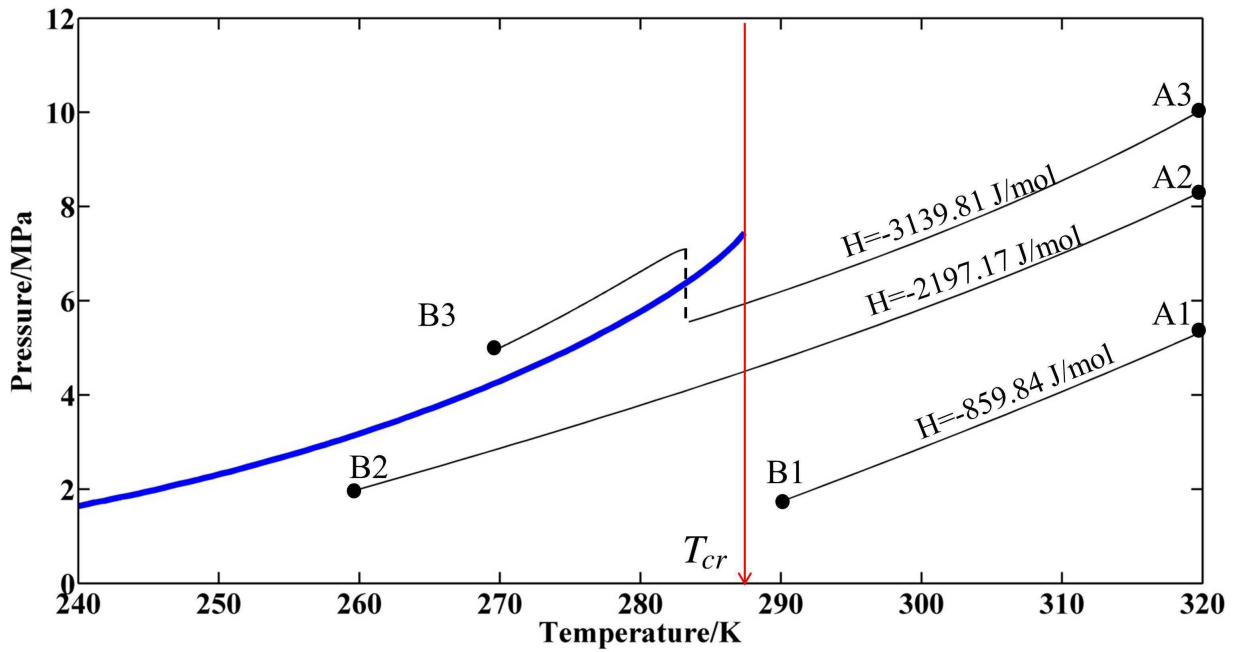


Figure 2: A diagram illustrating isenthalpic expansion for a mixture of methane and CO<sub>2</sub> with a constant total mole fraction of CO<sub>2</sub> of  $y_{\text{FCO}_2} = 0.8$ . The arrow denotes the criconden-therm,  $T_{cr}$ . The thick solid curve denotes the dew pressure as a function of temperature, as calculated using the SAFT- $\gamma$  Mie equation of state<sup>47</sup>. Isenthalpic curves (thin solid curves) denote adiabatic expansions from three points A<sub>i</sub>,  $i=1,2,3$  to three points B<sub>i</sub>,  $i=1,2,3$ .

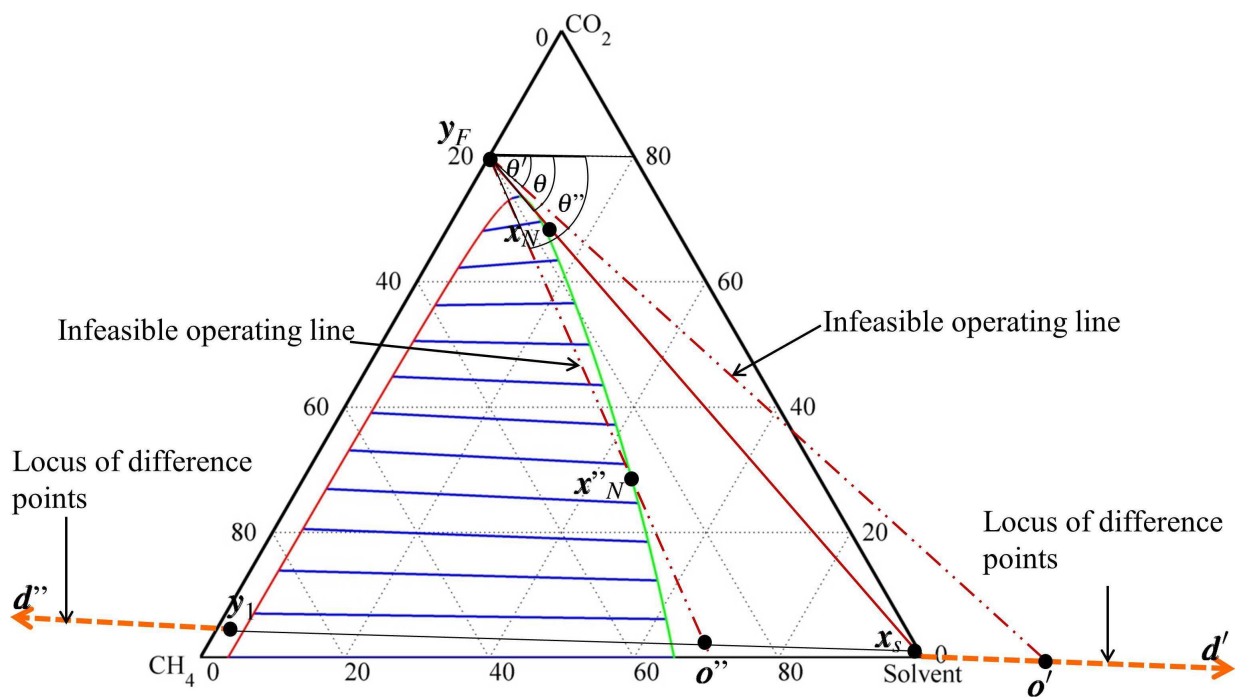


Figure 3: A phase diagram for CO<sub>2</sub>-methane-solvent (propyl-methyl ether) at  $T_N = 304.4$  K,  $P_{abs} = 9.0$  MPa, illustrating the locus of difference points (dashed lines, points  $d'$ ,  $d''$ ,  $o'$  and  $o''$ ) and infeasible operating lines as discussed in the text.  $y_1$  is the composition of the gas stream leaving the absorber,  $y_F$  the composition of the feed stream entering the absorber and  $x_s$  the composition of the pure solvent stream entering the absorber.

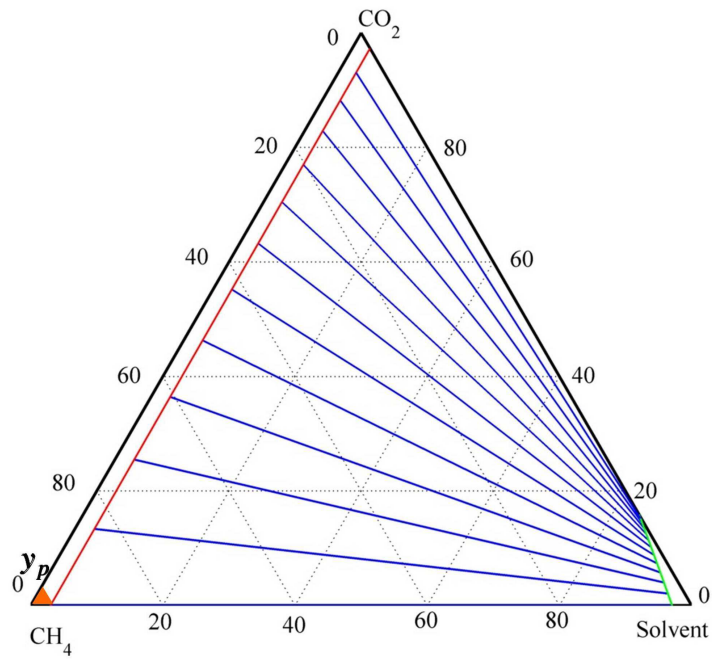
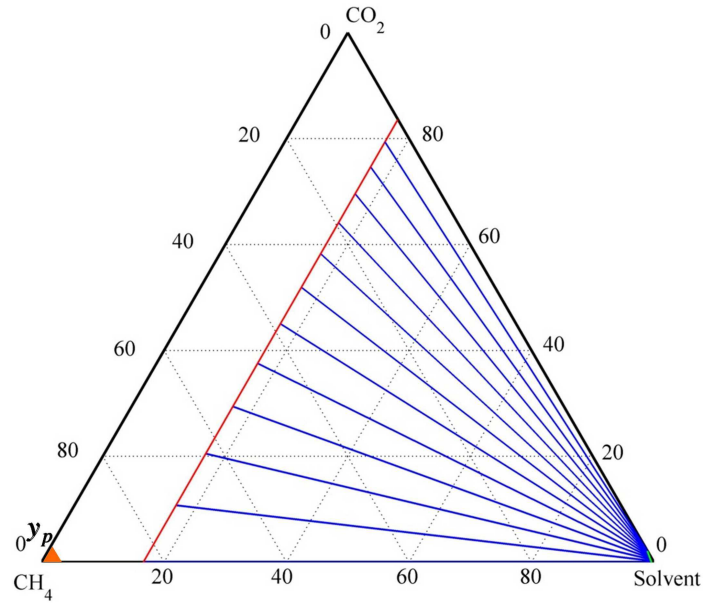


Figure 4: Phase diagram for CO<sub>2</sub>-methane-solvent (propyl-methyl ether) at  $T_1 = 270$  K and pressure  $P_1$ . a)  $P_1 = 0.1$  MPa. b)  $P_1 = 0.610$  MPa. The shaded region represents  $y_{1,1} \geq y_p = 0.97$

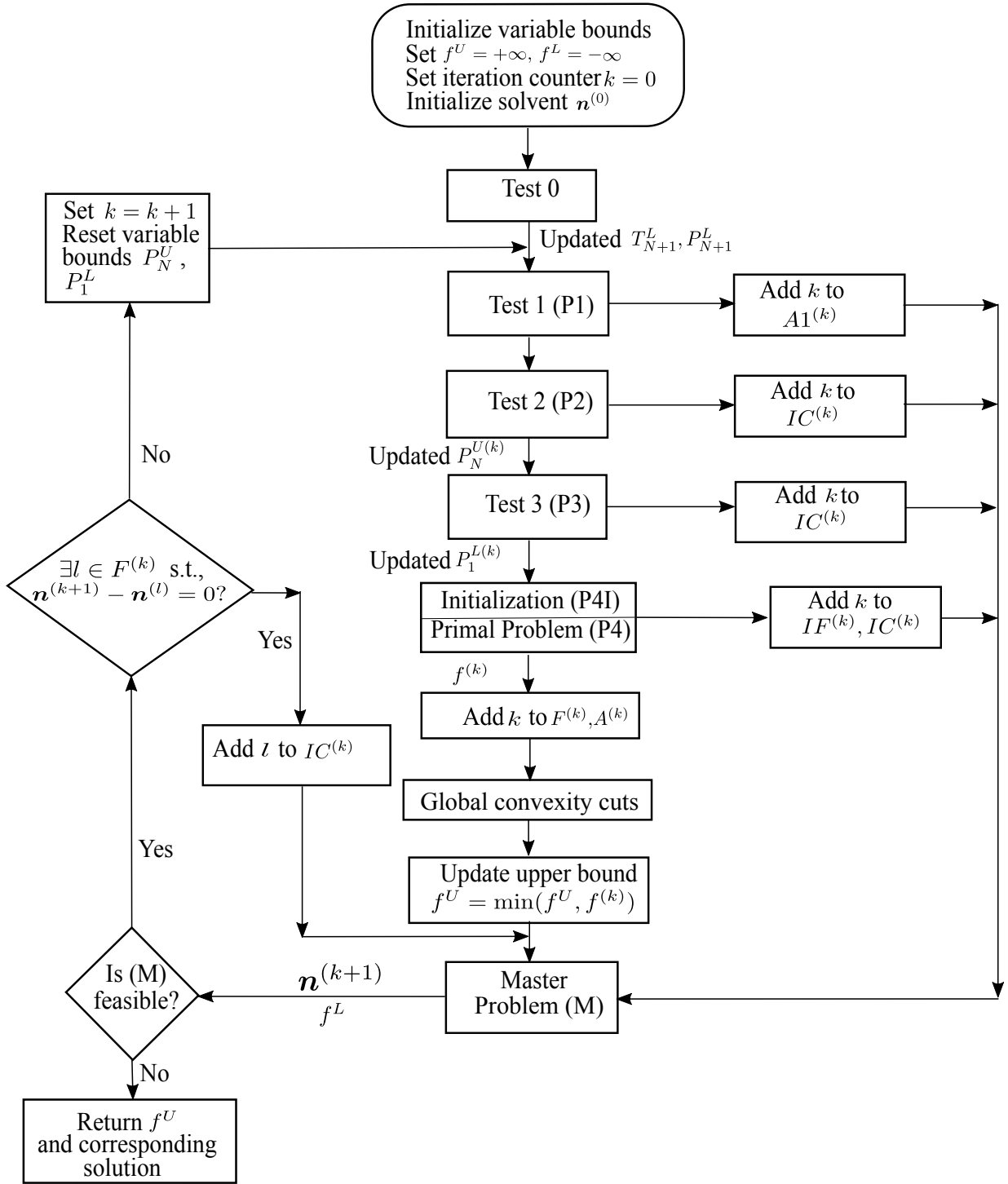


Figure 5: A flowchart of the proposed algorithm.



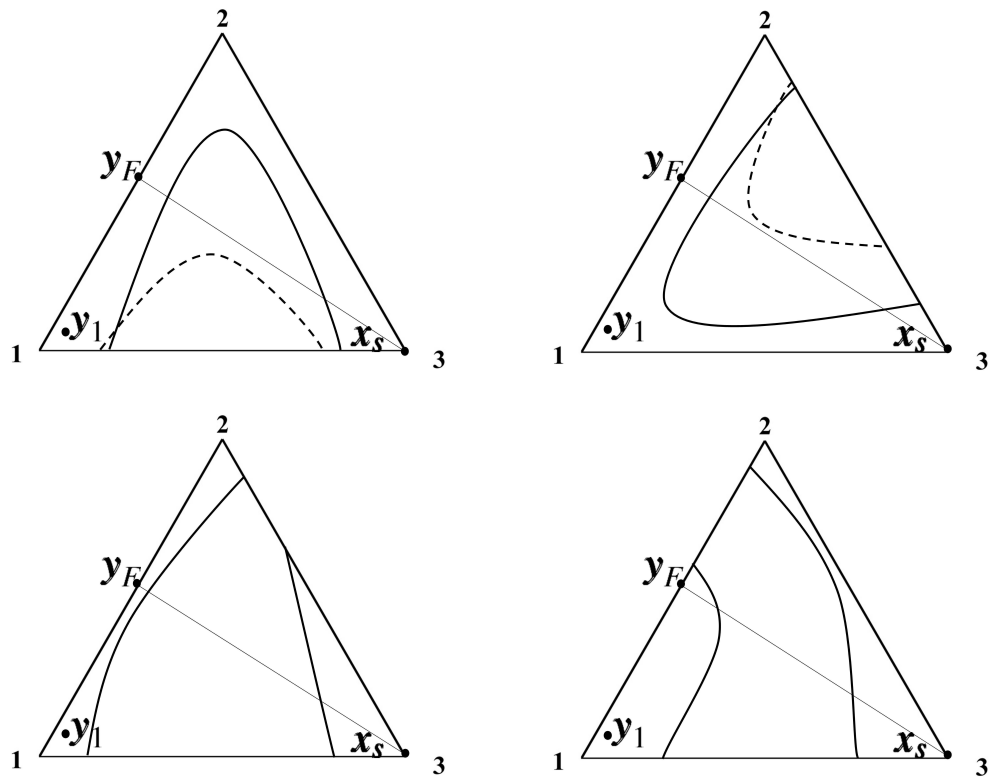


Figure 6: Four types of ternary phase diagrams for a product (1), solute (2) and solvent (3) at constant pressure and temperature. a) The solvent and product pair is partially miscible and other pairs are fully miscible; b) The solvent and solute pair is partially miscible and other pairs are fully miscible; c) The solvent and solute pair is partially miscible and the solvent and product pair is partially miscible; d) The product and solute pair is partially miscible and the solvent and product pair is partially miscible.  $y_F$  denotes the feed composition,  $y_1$  denotes the product composition and  $x_s$  the lean solvent composition. The thick curves denote the vapour-liquid envelope at pressure  $P$ . The dashed curves indicate the vapour-liquid envelope at a pressure  $P'$ , such that  $P > P'$ .